Rbfox3-regulated alternative splicing of Numb promotes neuronal differentiation during development

Kee K. Kim,[1] Joseph Nam,[2] Yoh-suke Mukouyama,[2] and Sachiyo Kawamoto[1]

[1]Laboratory of Molecular Cardiology and [2]Laboratory of Stem Cell and Neuro-Vascular Biology, National Heart, Lung, and Blood Institute, National Institutes of Health, Bethesda, MD 20892

Alternative premRNA splicing is a major mechanism to generate diversity of gene products. However, the biological roles of alternative splicing during development remain elusive. Here, we focus on a neuron-specific RNA-binding protein, Rbfox3, recently identified as the antigen of the widely used anti-NeuN antibody. siRNA-mediated loss-of-function studies using the developing chicken spinal cord revealed that Rbfox3 is required to promote neuronal differentiation of postmitotic neurons. *Numb* premRNA encoding a signaling adaptor protein was found to be a target of Rbfox3 action, and Rbfox3 repressed the inclusion of an alternative exon via binding to the conserved UGCAUG element in the upstream intron. Depleting a specific Numb splice isoform reproduced similar neuronal differentiation defects. Forced expression of the relevant Numb splice isoform was sufficient to rescue, in an isoform-specific manner, postmitotic neurons from defects in differentiation caused by Rbfox3 depletion. Thus, Rbfox3-dependent *Numb* alternative splicing plays an important role in the progression of neuronal differentiation during vertebrate development.

Introduction

Alternative splicing is an essential mechanism for the post-transcriptional regulation of gene expression and for the diversification of gene products. Sequence-specific RNA-binding proteins govern mechanisms that activate and repress splice sites, or modulate exon or intron definition. Among them, the RNA-binding Fox (Rbfox) family has recently been characterized as phylogenetically conserved regulators of alternative splicing (Jin et al., 2003; Nakahata and Kawamoto, 2005; Underwood et al., 2005; Ponthier et al., 2006; Kuroyanagi et al., 2007; Kim et al., 2009). Rbfox protein contains a single conserved RNA recognition motif (RRM)–type RNA-binding domain in the central region of the molecule and binds specifically to an RNA penta(hexa)nucleotide (U)GCAUG. Rbfox protein can function as an activator and a repressor of alternative splicing depending on its binding location on premRNA relative to the regulated exon. Rbfox proteins enhance exon inclusion by binding to the (U)GCAUG element that lies downstream of the alternative exon, whereas they repress exon inclusion by binding to the same element upstream of the alternative exon (Jin et al., 2003; Yeo et al., 2009).

The Rbfox family in mammals consists of three members, Rbfox1 (also known as Fox-1 or A2BP1), Rbfox2 (Fox-2, Rbm9, or Fxh), and Rbfox3 (Fox-3, D11Bwg0517e, or NeuN). Rbfox1 is expressed in neurons, heart, and skeletal muscle myocytes, whereas Rbfox2 is widely expressed in various tissues and cell types including neurons and embryonic stem cells. In contrast, Rbfox3 expression is restricted to neurons (McKee et al., 2005; Kim et al., 2009). Of note is our recent discovery that Rbfox3 is actually the antigen of the anti-NeuN antibody (Kim et al., 2009), which has served as a reliable neuronal nuclear marker for 20 years in vertebrate development and differentiation of stem cells (Mullen et al., 1992). The vertebrate central nervous system (CNS) expresses all three Rbfox proteins. This may contribute to highly abundant alternative splicing in the CNS relative to other tissues. Many genes participating in neurogenesis, axon guidance, synapse formation, and neurological activities are known to generate alternatively spliced isoforms. Some of them are candidate targets of Rbfox regulation. How Rbfox-mediated

Correspondence to Yoh-suke Mukouyama: mukoyamay@mail.nih.gov; or Sachiyo Kawamoto: kawamots@mail.nih.gov

Abbreviations used in this paper: CNS, central nervous system; E, embryonic day; MZ, marginal zone; pNF, phosphorylated neurofilaments; PRR, proline-rich region; RRM, RNA recognition motif; UIS, upstream intronic silencer; VZ, ventricular zone.

The Rockefeller University Press $30.00
J. Cell Biol. Vol. 200 No. 4 443–458
www.jcb.org/cgi/doi/10.1083/jcb.201206146

splicing events influence the development and physiology in the CNS is largely unknown (Gehman et al., 2011, 2012).

The embryonic spinal cord has been studied intensively in order to understand the mechanisms underlying CNS development. This program begins with the subtype specification of progenitor cells located at defined positions along the dorsoventral axis in the ventricular zone (VZ; Jessell, 2000; Briscoe and Novitch, 2008). Specification of progenitor subtypes depends on coordinated morphogen gradients that trigger the combinatorial expression of different basic-helix-loop-helix and homeodomain transcription factors. These committed progenitors exit the cell cycle and differentiate into a diverse set of neurons with distinct neurotransmitter properties. Although the biological significance of transcriptional regulation during spinal cord neuronal development has been well established, additional mechanisms may also contribute to the precise regulation of transcription factors and signaling molecules.

Here, we consider the role of alternative splicing regulation by Rbfox3 in neuronal differentiation of cultured cells and the developing spinal cord. We propose that Rbfox3-dependent alternative splicing of *Numb*, which encodes a signaling adaptor protein, drives postmitotic neurons to advance a differentiation process during development.

Results

Rbfox3 is required for neuronal differentiation of mouse P19 cells

We have previously shown that Rbfox3 is induced during neuronal differentiation of mouse embryonic carcinoma–derived P19 cells triggered by retinoic acid treatment (Kim et al., 2009, 2011). To examine whether Rbfox3 is required for neuronal differentiation in vitro, we used an shRNA-mediated knockdown system in culture. Two shRNAs, *shRbfox3-T2* and *shRbfox3-T3*, which target two different regions of *Rbfox3* mRNAs were used to inhibit Rbfox3 expression. GFP shRNA (*shGFP*) serves as a negative control. In *shGFP*-expressing P19 cells, induction of Rbfox3 is accompanied by outgrowth of neurites and/or long axon-like extensions, which contains an axonal marker, phosphorylated neurofilaments (pNF; Fig. 1, A, G, and J, arrowheads). The shRNA-mediated knockdown of Rbfox3 results in a decrease in axon-like extensions and an almost complete elimination of pNF (Fig. 1, B, C, E, F, H, I, K, and L). These observations are also supported by immunoblot data shown in Fig. 1 M. To assess the specificity of the Rbfox3 knockdown phenotype, *shRbfox3-T2*–expressing cells were transfected with rescue constructs encoding two mouse *Rbfox3* isoforms, *Rbfox3-L* and *-S*, with silent mutations so as not to anneal with *shRbfox3-T2*. Rbfox3-L and -S, both of which contain the RRM, are identical except that Rbfox3-L including a 47 aa-insertion in the C-terminal region. Consistent with previous observations that both Rbfox3-L and -S are capable of activating neural cell–specific alternative splicing (Kim et al., 2009), both isoforms increase pNF (Fig. 1 N). These results suggest that Rbfox3 is required for neuronal differentiation of P19 cells.

Identification and characterization of chicken Rbfox3

To study a role for Rbfox3 in neuronal development in vivo, we chose the chicken embryonic neural tube because of the ease of electroporation and because spinal neuronal development has been characterized most extensively in this species. To make use of the chick neural tube for in vivo loss-of-function and gain-of-function experiments, we first sought to identify the chicken orthologue of mammalian *Rbfox3* because the current chicken genome database does not include a sequence annotated for *Rbfox3*. At least two splice variants for the *Rbfox3* coding sequence, *full-length Rbfox3 (Rbfox3-full*) and *Rbfox-3 with a 31 aa deletion* (*Rbfox3-d31*), were found using RNAs isolated from embryonic day 5 (E5) embryos. The two sequences are identical except for a 93-nt cassette exon (93-nt RRM exon) encoding 31 aa, which is included in *Rbfox3-full* but is excluded in *Rbfox3-d31* (Fig. 2 A). This 31-aa sequence is a part of the RRM and includes a critical ribonucleoprotein consensus element, RNP1, necessary for RNA binding (Maris et al., 2005; Auweter et al., 2006). Therefore, Rbfox3-d31 lacks both the structure and function of the RRM. On the other hand, Rbfox3-full contains the intact RRM, which is almost identical (76/77 aa identity) to the RRM of mouse Rbfox3 (Fig. S1 A). Overall, chicken Rbfox3-full and mouse Rbfox3 share a 92% aa sequence identity. Of note is that the very N-terminal 1–20 aa sequence of chicken Rbfox3 is 100% identical to that of mouse Rbfox3, where an epitope of anti-NeuN (hereafter designated anti-Rbfox3) is localized (Fig. S1, B and C; Dredge and Jensen, 2011).

We then characterized the two chicken Rbfox3 isoforms. Rbfox3-d31 protein, unlike Rbfox3-full, is highly susceptible to degradation via a MG132-sensitive proteasome pathway (Fig. S1 G, bottom panel, bottom row). We also examined whether these chicken Rbfox3 isoforms were able to regulate alternative splicing. To test this, we used the neural cell–specific alternative splicing of exon N30 in the *nonmuscle myosin heavy chain II-B* gene as a model (Nakahata and Kawamoto, 2005). The UGCAUG element is located in the intron downstream of N30 (Fig. S1 G, top panel). N30 inclusion is up-regulated by exogenous expression of Rbfox3-full, whereas Rbfox3-d31 fails to activate N30 splicing despite its stable expression in the presence of a proteasome inhibitor, MG132 (Fig. S1 G, bottom panel, middle row). These data suggest that Rbfox3-full and Rbfox3-d31 have different protein stabilities as well as different activities with respect to splicing regulation.

Expression of Rbfox3 in chick neural tube

We next examined the expression of *Rbfox3* mRNA in chicken embryos at different stages of development. RT-PCR analysis revealed that *Rbfox3* is expressed as early as E2, but essentially as the *Rbfox3-d31* variant (Fig. 2 B). Over the next few days, the expression of the *Rbfox3-d31* variant declines, whereas the *Rbfox3-full* variant increases (Fig. 2 B). We further analyzed the expression of chicken Rbfox3 protein. At E2, anti-Rbfox3 faintly detects two protein bands with M_r of 39 kD (arrowhead) and 43 kD (Fig. 2 C, top). Expression of the 43-kD isoform increases from E2 onward, whereas expression of the 39-kD isoform decreases. Taking into account the fact that the splicing

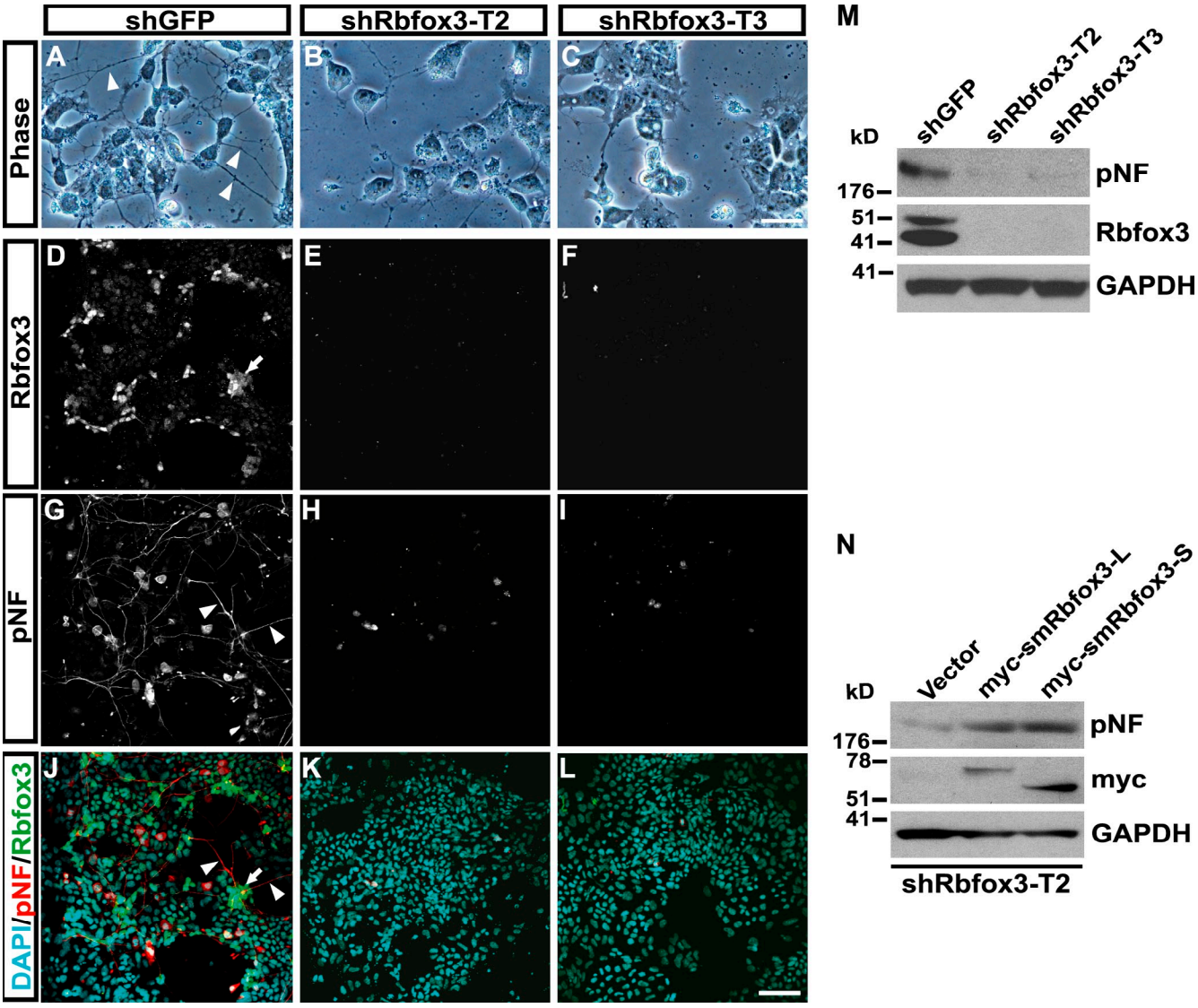

Figure 1. **Inhibition of neuronal differentiation of P19 cells by Rbfox3 knockdown.** (A–L) Decreased axonal outgrowth in Rbfox3 knockdown cells. P19 cells expressing shRNAs indicated at the top were treated with retinoic acid. Phase-contrast images and immunostaining for proteins indicated on the left are shown. Overlay image includes nuclear staining (DAPI). Arrowheads and an arrow indicate axonal processes and Rbfox3$^+$ cells, respectively. Bars: (C) 50 µm; (L) 100 µm. (M) Immunoblot analysis of Rbfox3 and pNF. GAPDH serves as a loading control. (N) Rescuing the effects of Rbfox3 shRNA by exogenous expression of Rbfox3 containing silent mutations. The expression constructs for myc-smRbfox3-L and -S contain silent mutations in the region targeted by *shRbfox3-T2*. Immunoblots detecting proteins indicated at the right are shown.

pattern of the 93-nt RRM exon changes from *Rbfox3-d31* to *Rbfox3-full* during embryonic development and the fact that the Rbfox3-d31 protein is much more unstable than Rbfox3-full in cells, the 43- and 39-kD isoforms most likely represent Rbfox3-full and Rbfox-d31, respectively. Importantly, the increase in the 43-kD Rbfox3 expression is accompanied by an increase in expression of neuron-specific class III β-tubulin (Tuj1, Fig. 2 C). In contrast, Rbfox2 is constantly expressed through development.

Next, we examined the expression of Rbfox3 in chick neural tube using anti-Rbfox3 in combination with DAPI, a nuclear dye. At E2, Rbfox3 expression is detected in only a few cells (per transverse section) located at the outer margin of the VZ (Fig. 2 D). At E3, the time at which the neural tube begins to generate postmitotic neurons in the lateral ventral region, Rbfox3 expression is confined to those neurons (Fig. 2 E). At E4 and E5, most postmitotic neurons in the expanded marginal zone (MZ) express Rbfox3 (Fig. 2, F and G). The number of Rbfox3$^+$ cells increases greatly from E3 to E4. In contrast, Rbfox3 protein is not detectable in VZ progenitor cells at any embryonic stages. These observations were confirmed in mice (Fig. S1, D–F).

We precisely defined the pattern of Rbfox3 expression in the ventral neural tube where early motor neuron differentiation occurs. Within the ventral one third of the neural tube, expression of the basic-helix-loop-helix transcription factor Olig2 persists in the VZ progenitor domain (pMN domain). Staining for p27kip1 (cyclin-dependent kinase inhibitor p27) sharply separates postmitotic cells from these progenitor cells (Fig. 2 H). While the homeodomain transcription factor MNR2 is expressed

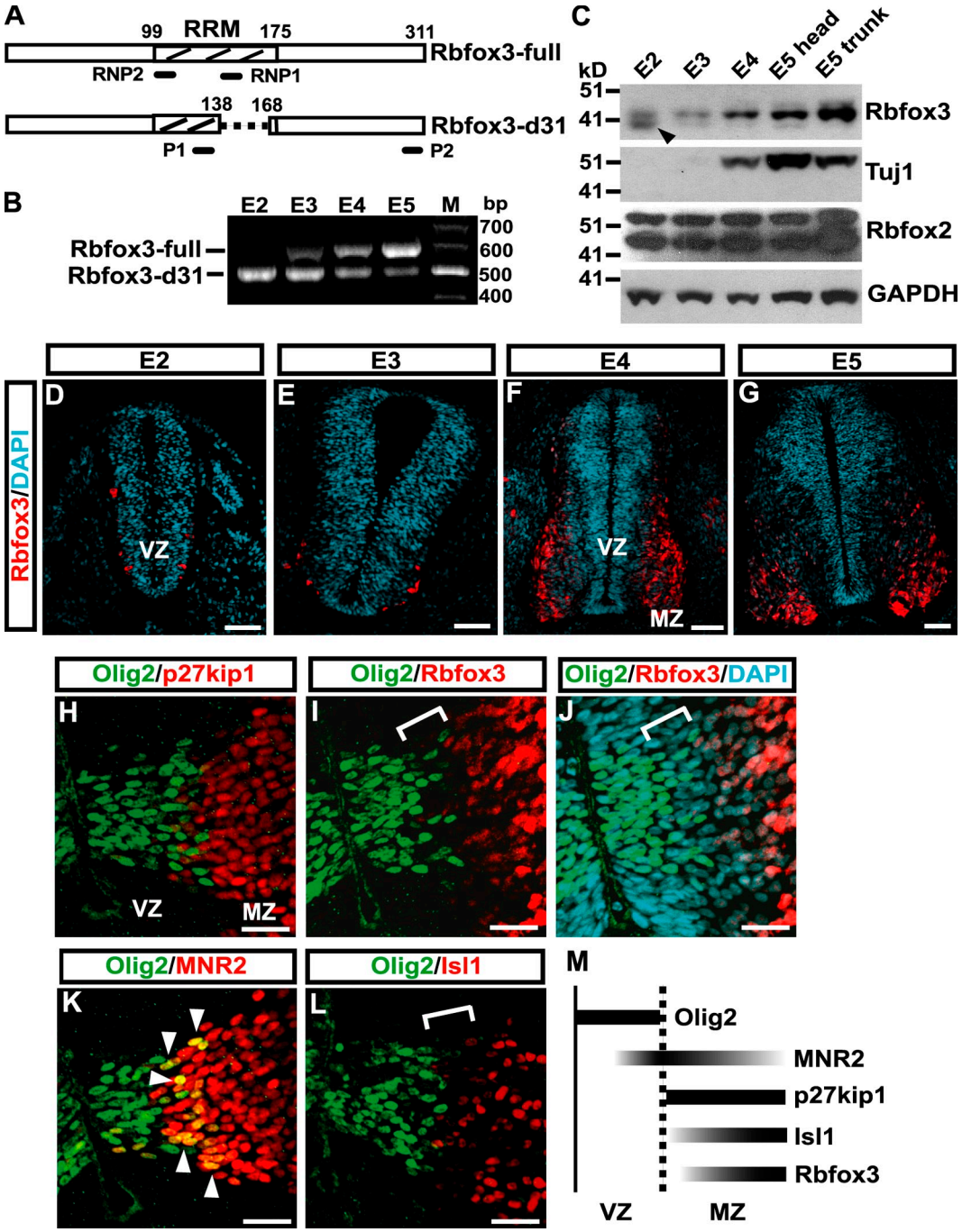

Figure 2. **Chicken Rbfox3 isoforms and their expression in chick neural tube.** (A) Diagrams of two alternatively spliced isoforms of Rbfox3. The dashed line indicates the deletion of 31 aa. Numbers represent aa. Two critical elements, RNP1 and RNP2, of the RRM for RNA binding are indicated. (B) Developmentally regulated expression of splice variants of *Rbfox3* mRNAs. mRNAs isolated from the embryos at the indicated embryonic days were analyzed by RT-PCR using primers P1 and P2 indicated in A. An ethidium bromide stained agarose gel is shown. M, size marker. (C) Developmentally regulated expression of Rbfox3 proteins. Embryonic extracts harvested at the indicated embryonic days were analyzed by immunoblotting for the indicated proteins. The top and bottom (indicated by an arrowhead) bands of Rbfox3 (top) presumably represent Rbfox3-full and Rbfox3-d31, respectively. (D–G) Expression of Rbfox3 protein in the developing chick neural tube. The transverse sections of the neural tube at the indicated embryonic days were stained with anti-Rbfox3 (red) and DAPI (cyan). Bars, 50 µm. (H–L) Restricted expression of Rbfox3 in late postmitotic neurons. Transverse sections of the E4 neural tube were stained for proteins indicated at the top. Brackets in I, J, and L indicate the areas where double-negative cells exist. Arrowheads in K indicate double-positive cells. Bars, 20 µm. (M) A schematic diagram to illustrate the time of the onset of expression and the localization of Rbfox3 and the marker proteins in the ventral neural tube at E4. A vertical solid line and a dashed line indicate the ventricular surface and the time point of cell cycle exit, respectively. The gradient gray scales represent the relative expression levels.

in laterally positioned Olig2$^+$ progenitors (Fig. 2 K, arrowheads) as well as in postmitotic motor neurons, the LIM homeodomain transcription factor Isl1 is expressed in more laterally positioned postmitotic motor neurons (Fig. 2 L). These staining patterns agree with previous studies showing that the expression of MNR2 begins during the final cell cycle of motor neuron progenitors

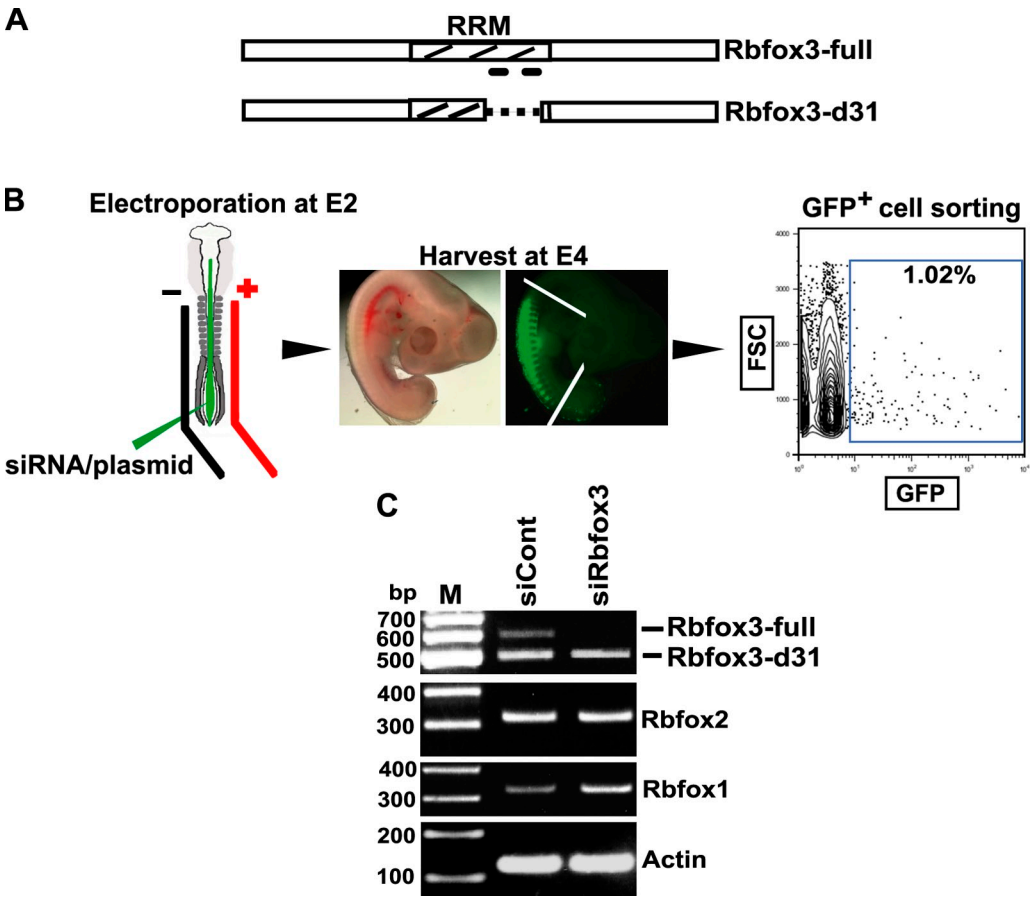

Figure 3. **Specific and efficient knockdown of *Rbfox3* by siRNAs.** (A) Location of the siRNAs specifically targeting *Rbfox3-full*. Two bars under *Rbfox3-full* indicate the regions targeted by the siRNAs (*siRbfox3*). (B) Schematic outline of the strategy to isolate transfected cells from embryos. Neural tube electroporation with siRNAs and the *GFP* expression construct (left), visualization of GFP signal in an embryo (middle), and FACS of the dissociated embryonic cells (right) are shown. Before cells are dissociated from the embryo, its head and tail were trimmed away (white lines in the middle panel). Typically ~1% of total dissociated cells are GFP$^+$. FSC, forward scatter. (C) Specificity of *siRbfox3* for *Rbfox3-full*. Total RNAs isolated from the GFP$^+$ cells electroporated with indicated siRNAs were analyzed by RT-PCR for the indicated mRNAs. *Actin* mRNA serves as a control. Because the data in panel C of this figure and Fig. 7 A were from the same experiment, the "Actin" panels in these two figures are the same.

whereas the Isl1 expression takes place after complete exit of the cell cycle (Tanabe et al., 1998). Expression of Rbfox3 is detected in lateral postmitotic motor neurons, similar to Isl1 expression, a short distance (bracket) from the Olig2$^+$ motor neuron progenitors (Fig. 2, I, J, and L). Notably, expression of MNR2 and p27kip1 precedes that of Rbfox3 (Fig. 2, I vs. K, I vs. H; M), suggesting that Rbfox3 expression is confined to late postmitotic neurons and not to early postmitotic neurons.

Rbfox3-full expression is necessary for late neuronal differentiation

We next examined whether Rbfox3 plays an essential role in spinal neuronal development. To address this question, we focused on the intact RRM-containing Rbfox3-full isoform because expression of this isoform is associated with neuronal differentiation. To abolish only Rbfox3-full expression, we generated siRNAs to target the 93-nt region unique to *Rbfox3-full* (Fig. 3 A). Rbfox3 siRNAs (*siRbfox3*) or a nonspecific control siRNA (*siCont*) together with a control *GFP* expression plasmid were electroporated into the neural tube at E2, at the onset of neurogenesis in ovo. The effective and specific knockdown of endogenous *Rbfox3-full* mRNAs in E4 neural tube was verified by RT-PCR. The GFP$^+$ neural tube cells were isolated from the electroporated embryos by FACS (Fig. 3 B). *Rbfox3-full* mRNAs but not *Rbfox3-d31* mRNAs are efficiently eliminated in *siRbfox3*-electroporated cells (Fig. 3 C). *SiRbfox3* does not reduce the mRNA levels of other Rbfox family members, *Rbfox1* and *Rbfox2* (Fig. 3 C). The *Rbfox1* mRNA level appears to be increased. Furthermore, immunohistochemical analysis with anti-Rbfox3 demonstrates that compared with *siCont* electroporated neural tubes, there is a greater than 75% reduction in Rbfox3 expression in the Rbfox3 knockdown embryos (Fig. 4, C vs. D; quantitated in K). This reduction of Rbfox3$^+$ cells is not due to cell death because the total number of DAPI$^+$ nuclei in the *siRbfox3*-electroporated neural tubes appears unchanged at E4, and no significant increase in TUNEL$^+$ apoptotic cells or decrease of phospho-histone3$^+$ mitotic cells is observed (Fig. S2, U and V).

We then examined whether knockdown of Rbfox3-full influences spinal neuronal differentiation. Significant reductions in Lim1/2$^+$ interneurons (Fig. 4, E vs. F; K) and MNR2$^+$ (Fig. 4, G vs. H; K) and Isl1$^+$ (Fig. 4, I vs. J; K) motor neurons are observed in Rbfox3-full knockdown neural tubes. In addition, class III β-tubulin expression, a pan-neuronal axon marker, was

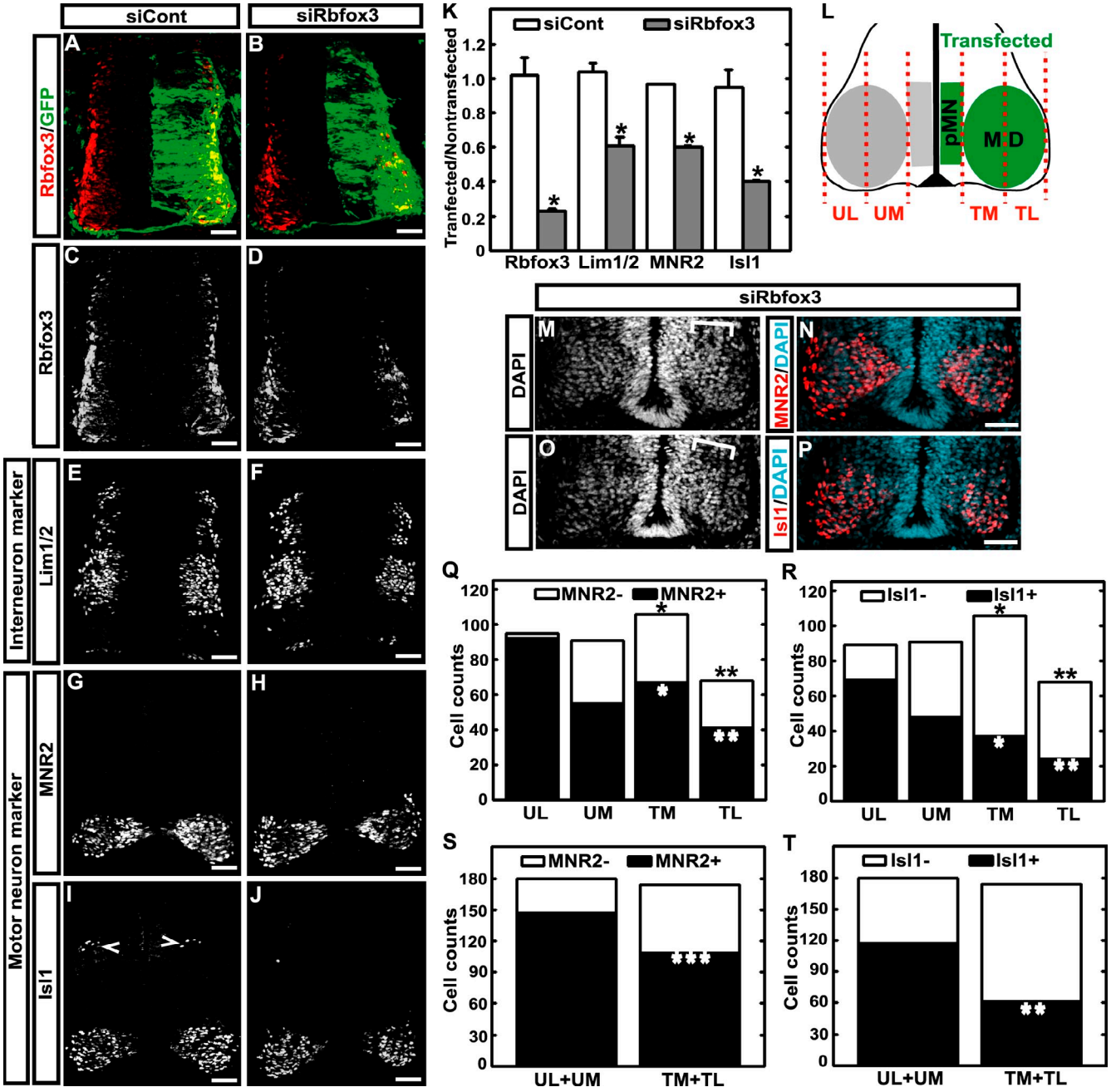

Figure 4. **Impaired neuronal differentiation after Rbfox3-full knockdown.** (A–J) Immunostaining of E4 neural tubes for Rbfox3 and neuronal markers. The right side of the neural tube in each panel has been transfected with siRNA indicated at the top and the *GFP* construct, as demonstrated by GFP in A and B. Sections were stained for proteins indicated on the left. Isl1$^+$ cells indicated by open arrowheads in I are D2 interneurons. Bars, 50 µm. (K) Quantification of marker$^+$ cells. Each bar represents the marker$^+$ cell number in the transfected side divided by those in the contra-lateral untransfected side, except for Rbfox3 (mean ± SD, 5 embryos, 3 sections/embryo). In the case of Rbfox3, the fluorescence intensity is used instead of marker$^+$ cell number. Isl1$^+$ cells in the D2 domain are not included for quantification. *, P < 0.0001 compared with *siCont* (*t* test). (L) Diagram of the ventral neural tube specifying four motor subdomains. The red dashed lines indicate the borders of the subdomains. The mid-lines are halfway between the borders of the motor domains. TM, transfected medial motor domain; TL, transfected lateral motor domain; UM, untransfected medial motor domain; UL, untransfected lateral motor domain; MD, motor domain; pMN, motor neuron progenitor domain. (M–P) Differential effects of Rbfox3 knockdown on expression of differentiation markers and cellular distribution in different regions of the motor domain. The right side of the neural tube has been transfected with *siRbfox3*. Brackets in M and O indicate the areas with higher cell density compared with the untransfected side. Bars, 50 µm. (Q–T) Quantification of cell numbers with and without expression of motor neuron markers. Detailed statistical values are provided in Fig. S2 T. *, P < 0.006; **, P < 0.003; ***, P < 0.03 compared with corresponding untransfected subdomain. Black and white asterisks are for total and marker$^+$ cell counts, respectively.

also decreased in the knockdown neural tubes (immunofluorescence intensity, 54 ± 6%, mean ± SD, $n = 5$). In the motor domains, interestingly, the reductions in MNR2$^+$ and Isl1$^+$ cells in the lateral region (Fig. 4 L, TL: transfected lateral motor domain, UL: untransfected lateral motor domain) appear more robust than the reduction in the medial motor domain (Fig. 4 L, TM: transfected medial motor domain, UM: untransfected medial motor domain; N and P quantitated in Q and R; TL/UL vs. TM/UM).

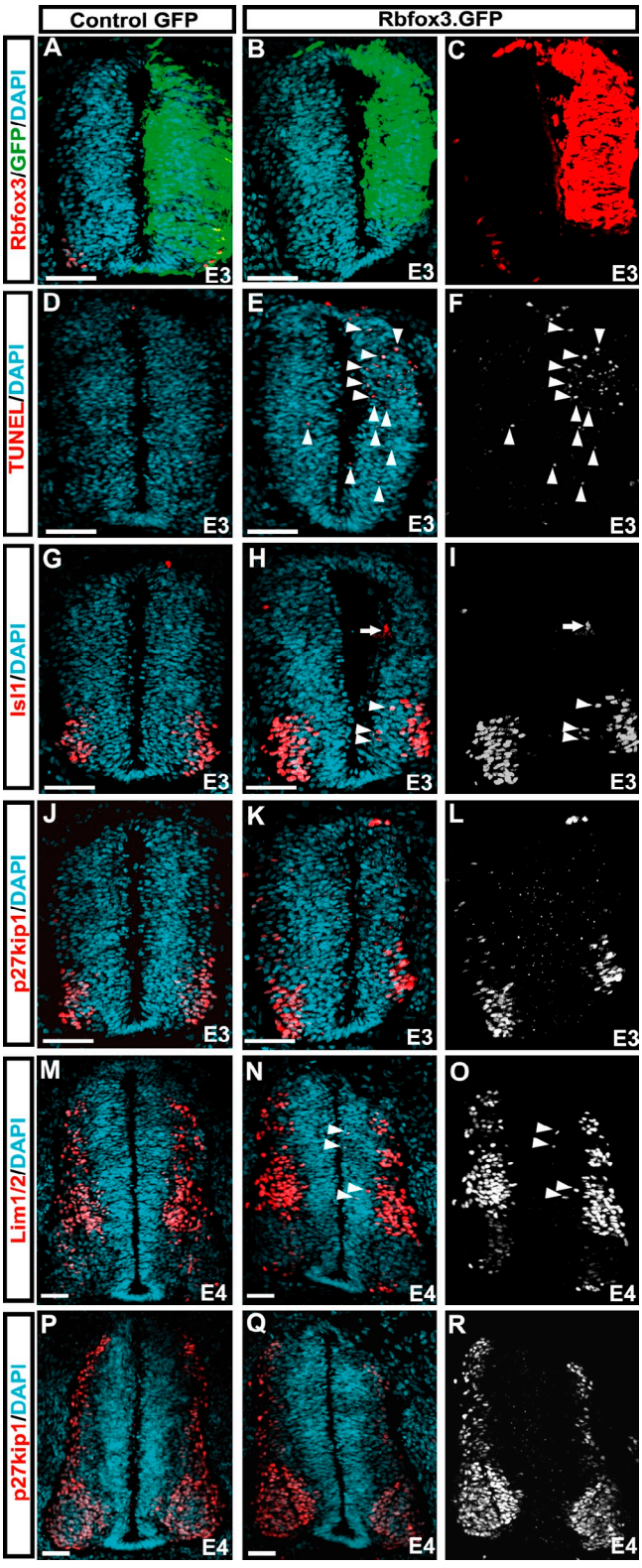

Figure 5. **Effects of forced expression of Rbfox3-full on progenitors in the VZ.** The expression constructs indicated at the top were transfected and sections of the neural tube were stained for markers indicated on the left and nuclei (DAPI). The right side in each panel is the transfected side, as demonstrated by GFP in A and B. A–L are E3 embryos, and M–R are E4 embryos. Arrowheads in E and F indicate some of the TUNEL$^+$ apoptotic cells. Arrowheads and an arrow in H and I indicate precocious expression of Isl1 in motor neuron progenitor and D2 neuron progenitor domains, respectively. Arrowheads in N and O indicate precocious expression of the interneuron marker Lim1/2 in the VZ. Expression of the postmitotic cell marker p27kip1 is not increased in the VZ (K, L, Q, and R). F, I, L, O, and R show only red fluorescence signals without DAPI, which is shown in E, H, K, N, and Q. Bars, 50 µm.

However, the total number of cells in the entire motor domain appears unaffected (Fig. 4, S and T; UL + UM vs. TM + TL). This may be possibly due to two effects of Rbfox3 depletion. First, the loss of Rbfox3-full alters the distribution of postmitotic cells in the motor domain. A significant increase in the cell number in the TM and a decrease in the cell number in the TL are seen in the knockdown neural tubes (Fig. 4, M and O, quantitated in Q and R; TM vs. UM, TL vs. UL). Second, knockdown of Rbfox3-full blocks motor neuron differentiation. There are robust reductions in MNR2$^+$ and Isl1$^+$ motor neurons in the TL, whereas a significant decrease in Isl1$^+$ cells but an increase in MNR2$^+$ cells are seen in the TM (Fig. 4, Q and R). The different effects of Rbfox3 knockdown on MNR2 and Isl1 expression in the medial motor domain can be explained by the observation that the onset of MNR2 expression precedes that of Rbfox3 (Fig. 2, I vs. K; M) while there is a similar expression timing for Isl1 and Rbfox3 (Fig. 2, I vs. L; M). This suggests that Rbfox3 may be required for late motor neuron differentiation but not for the onset of motor neuron differentiation.

The observation that the numbers of MNR2$^-$ and Isl1$^-$ cells increase in the lateral motor domains in the Rbfox3 knockdown neural tubes prompted us to examine whether these cells change their neuronal subtypes. Notably, no ectopic expression of Lim1/2 is detectable in the motor domain (Fig. 4 F). In addition, we do not observe any remaining expression of VZ progenitor markers such as Olig2, Nkx2.2, Nkx6.1, and Pax6 in the lateral regions (Fig. S2, E–L; quantitated in N). We also analyzed *NeuroD4* and *Neurogenin2* mRNA expression, which are normally enriched in the cells located in the intermediate zone (Lee and Pfaff, 2003). No significant changes are readily apparent (Fig. S2, O and P). A possible explanation is that Rbfox3 might play a role in a pathway inducing expression of neuronal differentiation markers, rather than inhibiting expression of proneural or early differentiation markers, in postmitotic neurons.

Effects of forced expression of Rbfox3-full on neural progenitors

We next examined whether Rbfox3 has a potential to induce neuronal differentiation of progenitor cells. To address this question, we asked whether forced expression of Rbfox3-full could accelerate the timing and/or increase the extent of neuronal differentiation in vivo. Forced expression of Rbfox3-full causes cell loss at E3, due to a significant increase in TUNEL$^+$ apoptotic cells (Fig. 5, E and F; arrowheads). The induction of cell death results in the reduction of the VZ progenitors without affecting subtype specification (Fig. S3). However, we consistently noticed a precocious expression of Isl1 and Lim1/2 in a subset of the VZ cells at E4 (Fig. 5, H, I, N, and O; arrowheads and arrows), whereas on the contra-lateral control side or in the control GFP expressing neural tube, such cells were never detected. Despite precocious expression of differentiated neuronal

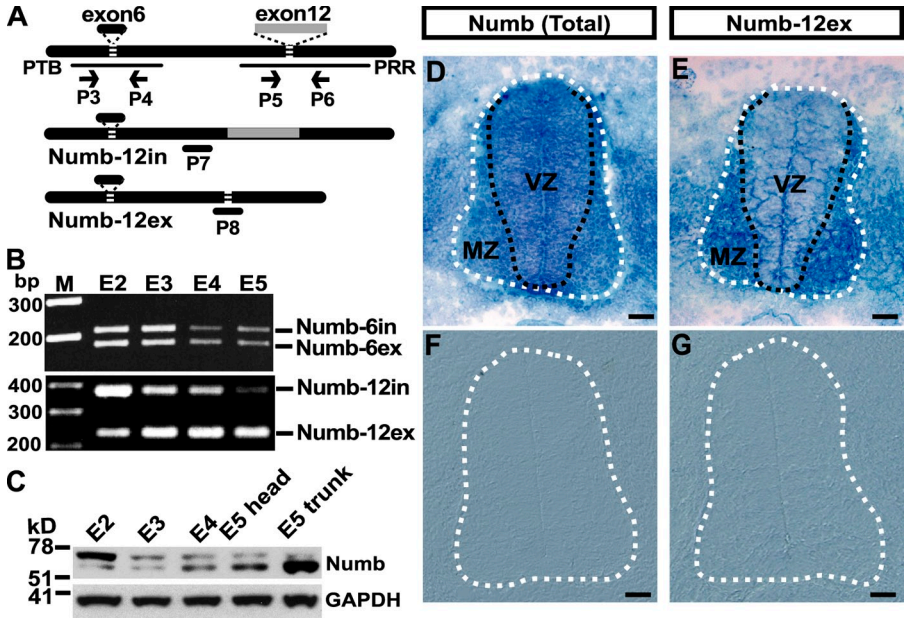

Figure 6. ***Numb* alternative splicing in the chick neural tube.** (A) Diagrams of chicken Numb splice isoforms. Locations of the regions encoded by two alternative exons, exon 6 and exon 12, are shown. Numb-12in and Numb-12ex includes and excludes exon 12, respectively. Two protein domains, phosphotyrosine-binding domain (PTB) and PRR, are indicated. P3–P6 indicate primers used for RT-PCR. P7 and P8 indicate in situ hybridization probes. (B) Developmental change in RNA splicing of *Numb* exon 6 and exon 12. The *Numb* mRNAs from embryos at the indicated times were analyzed by RT-PCR using primers P3 and P4 (A) for exon 6 (top) and P5 and P6 (A) for exon 12 (bottom). Numb-6in, Numb-exon 6 included; Numb-6ex, Numb-exon 6 excluded. (C) Developmental change in Numb protein isoform. Embryonic extracts harvested at the indicated times were analyzed by immunoblotting for Numb proteins. The top and bottom bands represent Numb-12in and Numb-12ex proteins, respectively. Each band most likely represents two proteins that include and exclude the 11 aa encoded by exon 6 but are not resolved under these electrophoresis conditions. (D–G) Restricted expression of the *Numb-12ex* splice variant to the MZ. In situ hybridization detecting total *Numb* mRNAs (D) using the common probe P7 (A) and that detecting the *Numb-12ex* splice variant (E) using the specific probe P8 (A) are shown. Hybridization-positive signals can be seen as dark blue staining. Sense strand probes complementary to P7 (F) and P8 (G) serve as negative controls. The spinal cord is outlined by a broken line. Bars, 50 µm.

markers, forced expression of Rbfox3-full does not induce the expression of the postmitotic marker p27kip1 in the VZ (Fig. 5, K, L, Q, and R). This suggests that Rbfox3-induced Isl1 or Lim1/2 expression in the VZ cells does not accompany cell cycle exit. These data suggest that, although Rbfox3-full is not sufficient to promote cell cycle exit when mis-expressed, it may nevertheless accelerate the timing for induction of neuronal differentiation markers.

Rbfox3-full regulates alternative splicing of *Numb* premRNA

To understand the mechanism by which Rbfox3-full regulates neuronal differentiation, we sought to determine the target gene(s) for which premRNA splicing is regulated by Rbfox3. Previous studies, using a number of strategies predicted sets of Rbfox-regulated exons (Zhang et al., 2008; Yeo et al., 2009). Among 74 mouse or human genes selected based on their potential participation in neuronal differentiation (Fagnani et al., 2007), we focused on 21 genes because conserved Rbfox-binding sites in the introns flanking alternative exons were confirmed in the currently available chicken genome sequence. We then performed semi-quantitative RT-PCR to examine whether changes in alternative splicing occur between E2 and E5 in chicken embryos. Although changes in percent inclusion (or exclusion) of an alternative exon from a number of genes were observed to some extent, only the *Numb* gene has an alternative exon (exon 12) for which the splicing pattern switched from included to excluded during neuronal development. A conserved TGCATG element is located in the intron just upstream of exon 12 and the chicken *Numb* gene contains an additional copy of the TGCATG element in tandem (Fig. S4 A). Exon 12 encodes 48 aa located within the proline-rich region (PRR) present in the C-terminal portion of the molecule (Fig. 6 A). A majority of *Numb* mRNAs include exon 12 at E2 (*Numb-12in*: exon 12–included Numb; Fig. 6 B, bottom). Over the next few days, the exon 12–excluded variant (*Numb-12ex*) becomes dominant. In contrast, the splicing pattern of another alternative exon, exon 6, which has no TGCATG element in its upstream or downstream introns, is not altered (Fig. 6 B, top). Immunoblot analysis using anti-Numb antibody, which detects all the splice isoforms, also shows a shift in the dominant Numb isoform from Numb-12in (~71 kD) to Numb-12ex (~65 kD) during development from E2 to E5 (Fig. 6 C). To determine where *Numb-12ex* is expressed in the chick neural tube, we analyzed localization of *Numb* mRNAs. In situ hybridization with a pan-probe for *Numb* mRNAs revealed that *Numb* mRNAs are expressed in the entire spinal cord at E4 (Fig. 6 D). Strikingly, a probe specific to the exon 12–excluded variants reveals that *Numb-12ex* mRNA is expressed at higher levels in the MZ (Fig. 6 E). This suggests that skipping exon 12 in *Numb* mRNAs occurs predominantly in the region where Rbfox3 is expressed.

We next examined whether Rbfox3 is responsible for alternative splicing of *Numb* during spinal neuronal development. Neural tubes were transfected with siRNAs and expression constructs, cells were isolated by FACS as shown in Fig. 3 B, and the *Numb* mRNA splicing pattern was analyzed. Knockdown of Rbfox3-full reduces exon 12 exclusion (Fig. 7 A), whereas forced expression of Rbfox3-full enhances exon 12 exclusion (Fig. 7 B). Thus, manipulation of Rbfox3-full expression influences *Numb* premRNA splicing in vivo. We further tested whether Rbfox3 binds to endogenous *Numb* premRNAs in vivo. After coimmunoprecipitation of Rbfox3-RNA complexes from E4 embryo extracts, the region including the UGCAUG element in intron 11 of *Numb* premRNA was amplified by RT-PCR. RNA–protein complexes pulled down by anti-Rbfox3, but not by nonspecific IgG, yield the predicted RT-PCR product (Fig. 7 C,

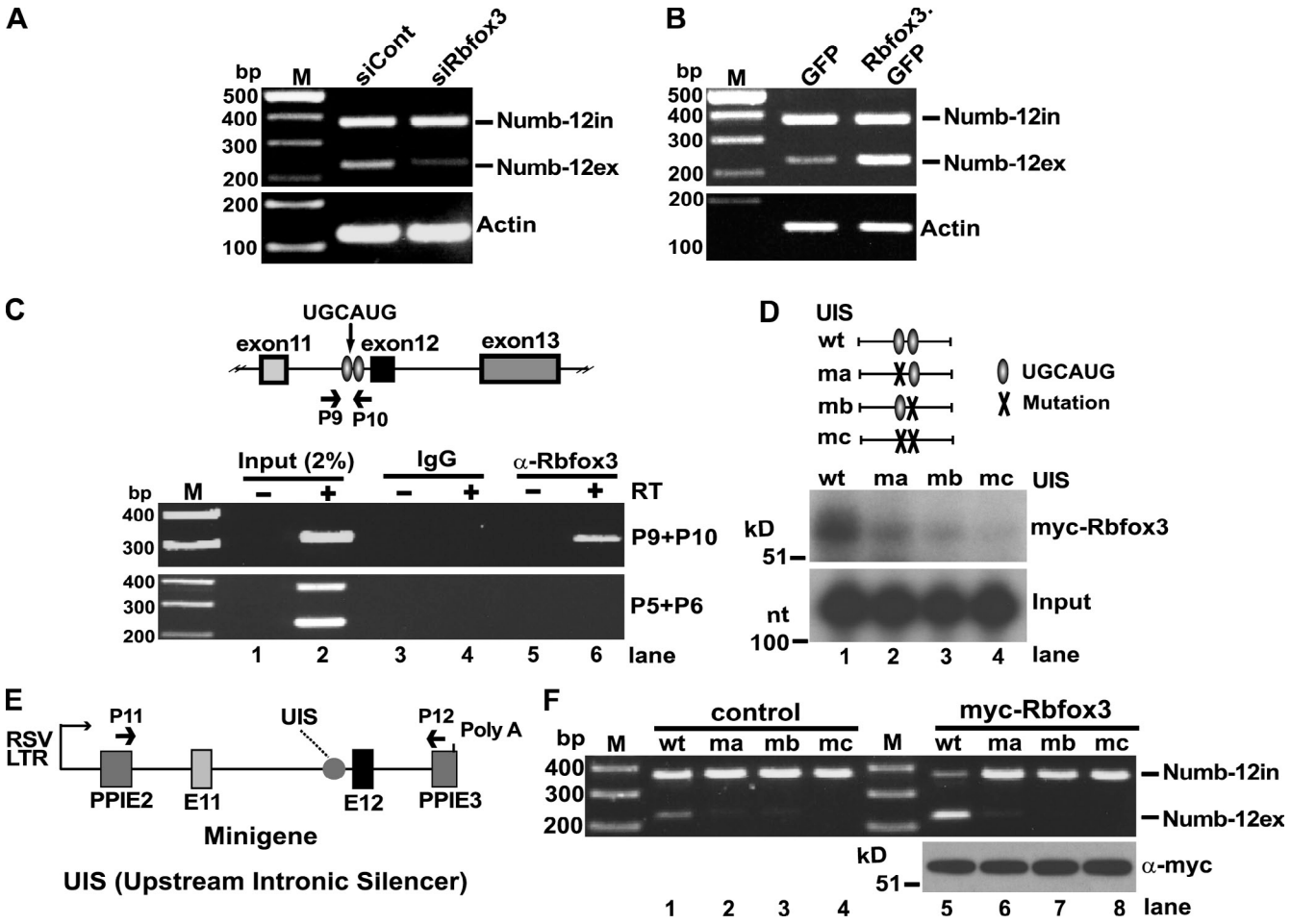

Figure 7. **Rbfox3 represses exon 12 of *Numb* via its direct binding to the UGCAUG elements in intron 11.** (A) Requirement for endogenous Rbfox3 for exclusion of exon 12 in *Numb* mRNAs. The indicated siRNAs were electroporated with the *GFP* construct in the neural tube at E2. GFP$^+$ cells were isolated by FACS from E4 embryos (see Fig. 3 B). The *Numb* mRNAs from GFP$^+$ cells were analyzed by RT-PCR. Because the data in Fig. 3 C and panel A of this figure were from the same experiment, the "Actin" panels in these two figures are the same. (B) Enhancement of *Numb* exon 12 exclusion by forced expression of Rbfox3-full. The *Rbfox3-full-ires-GFP* construct or the *GFP* construct was electroporated in the neural tube at E2. GFP$^+$ cells were isolated by FACS from E4 embryos. The *Numb* mRNAs from GFP$^+$ cells were analyzed by RT-PCR. (C) In vivo binding of Rbfox3 to *Numb* transcripts. Top: a diagram of the chicken *Numb* premRNA surrounding alternative exon 12. Exon 11 and exon 13 are constitutive exons. Rectangles and horizontal lines indicate exons and introns, respectively. Two copies of the UGCAUG element in intron 11 are shown as ovals. Bottom: detection of intron 11 of the *Numb* transcript associated with Rbfox3. E4 embryo extracts were subject to RNA–protein coimmunoprecipitation using the indicated antibodies. The intron 11 region of the *Numb* transcripts associated with the immunocomplex was analyzed by PCR (38 cycles) using primers P9 and P10 after incubation with reverse transcriptase (RT, +) or without RT (−). RT-PCR (33 cycles) of *Numb* mRNAs using primers P5 and P6 (see Fig. 6 A) serves as a negative control that lacks the UGCAUG element. (D) Direct binding of Rbfox3 to the UGCAUG elements of *Numb* intron 11 RNA in vitro. Top: a diagram of the upstream intronic silencers (UISs) in *Numb* intron 11 RNA, which includes wild-type or mutant UGCAUG elements. Bottom: after UV cross-linking of Rbfox3 with the indicated radiolabeled RNA probes, Rbfox3 was immunoprecipitated and subjected to SDS-PAGE. Autoradiography of SDS-PAGE (myc-Rbfox3) and input RNA probes after Urea-PAGE (Input) are shown. (E) A diagram of *Numb* minigene. The minigene includes the chicken *Numb* genomic DNA fragment containing exons E11 and E12 and intron 11, which are flanked by exons E2 and E3 of the rat *preproinsulin* gene (PPI). Transcription of the minigene is driven by the Rous sarcoma virus long terminal repeat (RSVLTR). Four different minigenes that contain the four different UISs, identical to the UISs shown in D (top), were constructed. (F) UGCAUG-dependent repression of exon 12 by Rbfox3. The minigenes containing the indicated UISs were cotransfected into SK-N-SH cells with the *Rbfox3* expression construct and exon 12 splicing patterns of the minigene mRNAs were analyzed by RT-PCR using primers P11 and P12 (E).

P9 + P10, lane 6). Absence of the PCR product in the RT-minus reaction (Fig. 7 C, P9 + P10, lane 5) excludes possible genomic DNA contamination. Further, absence of RT-PCR products using primers for an mRNA region which lacks the UGCAUG element (Fig. 7 C, P5 + P6, lane 6) is an indication that the Rbfox3–RNA complexes are specific to the UGCAUG element. These results indicate that Rbfox3 is recruited to intron 11 of *Numb* premRNAs in E4 embryos. Finally, we examined whether Rbfox3 is capable of directly regulating *Numb* exon 12 splicing. Direct binding of Rbfox3 to the UGCAUG elements in the context of the 146-nt upstream intronic silencer region (UIS) of intron 11 is shown using in vitro UV cross-linking of radiolabeled RNAs to in vitro–translated Rbfox3. The wild-type UIS, which contains two copies of the UGCAUG element binds strongly Rbfox3 (Fig. 7 D, lane 1). In contrast, mutant ma and mb, where one of the UGCAUG elements is mutated, bind to Rbfox3 to a lesser extent (Fig. 7 D, lanes 2 and 3). Binding of mutant mc, where both copies of the element are mutated, is almost undetectable (Fig. 7 D, lane 4). We further studied whether binding of Rbfox3 to the UGCAUG elements in intron 11 affects splicing of exon 12. To this end, we constructed a minigene which contains exon 11, the entire intron 11, exon 12, and short flanking regions of

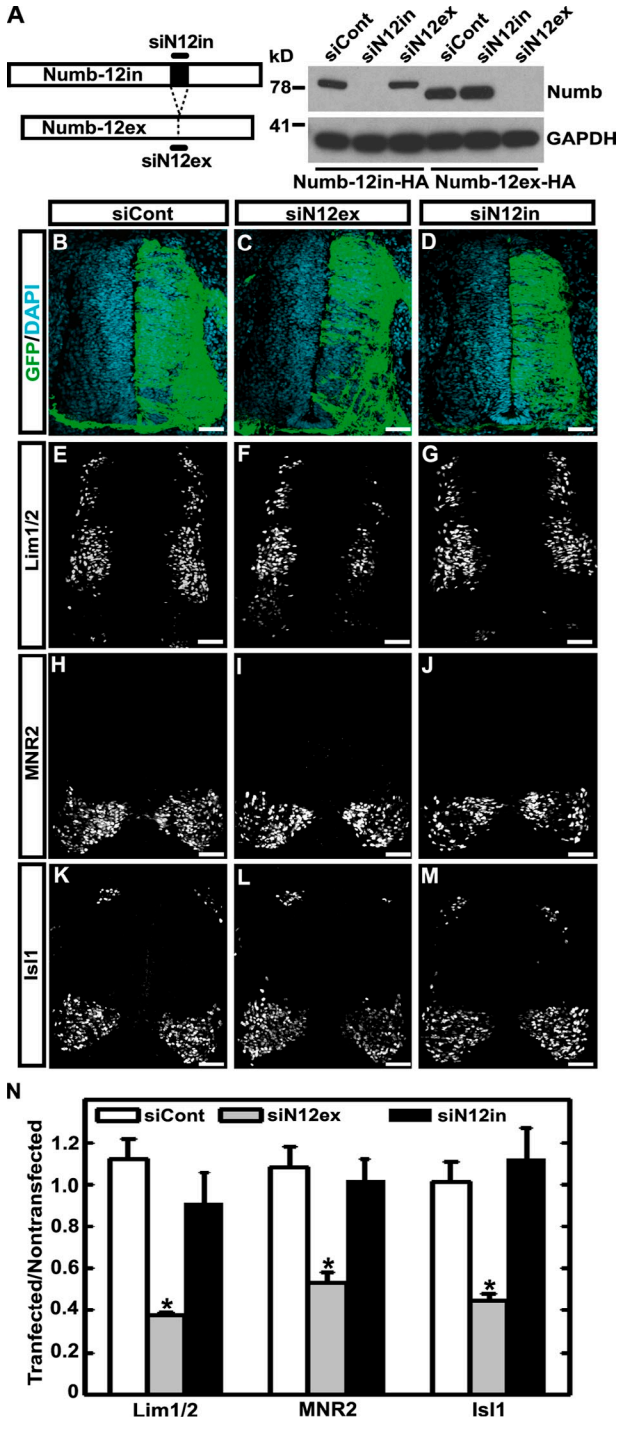

Figure 8. **Impaired neuronal differentiation by specific knockdown of Numb-12ex.** (A) Isoform specificity of siRNAs targeting *Numb*. Diagrams show the locations targeted by siRNAs specific for the *Numb-12in* mRNA (*siN12in*) and for the *Numb-12ex* mRNA (*siN12ex*). SiRNAs indicated at the top of the blots were transfected together with the expression constructs indicated at the bottom of the blots into P19 cells. Cell lysates were analyzed by immunoblotting using anti-Numb. (B–M) Immunostaining of the E4 neural tube for neuronal markers. The right side of the neural tube in each panel has been transfected with the indicated siRNA and the *GFP* construct, as demonstrated by GFP in B–D. Bars, 50 µm. (N) Quantification of marker$^+$ cells. Quantification was performed by the same procedure as Fig. 4 K (mean ± SD, 5 embryos, 3 sections/embryo). *, $P < 0.00005$ compared with *siCont*. There is no significant difference between *siCont* and *siN12in*.

the chicken *Numb* gene. This sequence was placed between exons 2 and 3 of the rat *preproinsulin* gene (Fig. 7 E). The mutant minigenes contained the same mutations in the UIS that was used for the in vitro cross-linking assay. These minigenes were transfected with the *Rbfox3* expression plasmid into the SK-N-SH neuroblastoma cell line, and the exon 12 splicing pattern of the minigenes was analyzed. Because the minigenes are chimeras of two genes, the mRNAs from the minigenes can be easily distinguished from the endogenous *Numb* mRNA. As shown in Fig. 7 F, exogenous Rbfox3 expression represses exon 12 inclusion in wild-type minigene mRNAs (Fig. 7, lane 1 vs. 5). No significant effect of Rbfox3 expression on the splicing patterns of mutant minigenes is seen (Fig. 7, lanes 6–8), indicating that Rbfox3 is capable of directly regulating exon 12 splicing in a UGCAUG-dependent manner, and that both copies of the UGCAUG element are required in this context. Repression of exon 12 splicing by various splice isoforms of mouse Rbfox3 was also examined (Fig. S4, B–D). Taken together, these data suggest that Rbfox3-full is responsible for exon 12 exclusion in *Numb* mRNAs via its direct binding to the upstream intronic UGCAUG element in chicken embryos.

Numb splicing switch by Rbfox3-full is required for neuronal differentiation

To address whether switching of the Numb splice isoform is required in spinal neuronal development, we performed an isoform-specific knockdown in chick spinal cord. Specific targeting of siRNAs to *Numb-12in* and *Numb-12ex* are shown in cultured cells transfected with the expression construct encoding each isoform (Fig. 8 A). In vivo knockdown of Numb-12ex reduces the number of Lim1/2$^+$ interneurons (Fig. 8, E vs. F; quantitated in N) and MNR2$^+$ and Isl1$^+$ motor neurons (Fig. 8, H vs. I, K vs. L; N), as previously observed for the Rbfox3-full knockdown embryos (Fig. 4). In contrast, knockdown of Numb-12in does not affect the expression of these differentiation markers (Fig. 8, E vs. G, H vs. J, K vs. M; N). These data indicate that *Numb* splicing to form Numb-12ex is required for spinal neuronal differentiation.

The above observation prompted us to explore whether forced expression of Numb-12ex is able to rescue the neuronal differentiation defects induced by Rbfox3-full knockdown. Forced expression of Numb-12ex by itself appeared not to affect VZ progenitor cell development and neuronal differentiation (Fig. S5, E, H, and K). Strikingly, co-electroporation of *siRbfox3* with the *Numb-12ex* expression construct effectively restored the numbers of Lim1/2$^+$ interneurons (Fig. 9, G vs. H; quantitated in P) and MNR2$^+$ and Isl1$^+$ motor neurons (Fig. 9, J vs. K, M vs. N; P). Importantly, Rbfox3 expression remained attenuated in the electroporated side (Fig. 9, D vs. E). Therefore, Numb-12ex functions downstream of Rbfox3 and a key role of Rbfox3 in spinal neuronal differentiation is induction of Numb-12ex expression. We also attempted to examine whether Numb-12in plays a role similar to Numb-12ex in neuronal differentiation. In contrast to Numb-12ex, forced expression of Numb-12in itself altered VZ progenitor development, resulting in the reduction in Lim1/2$^+$ interneurons and Isl1$^+$ motor neurons (Fig. S5, D vs. F, J vs. L). Co-electroporation of *siRbfox3*

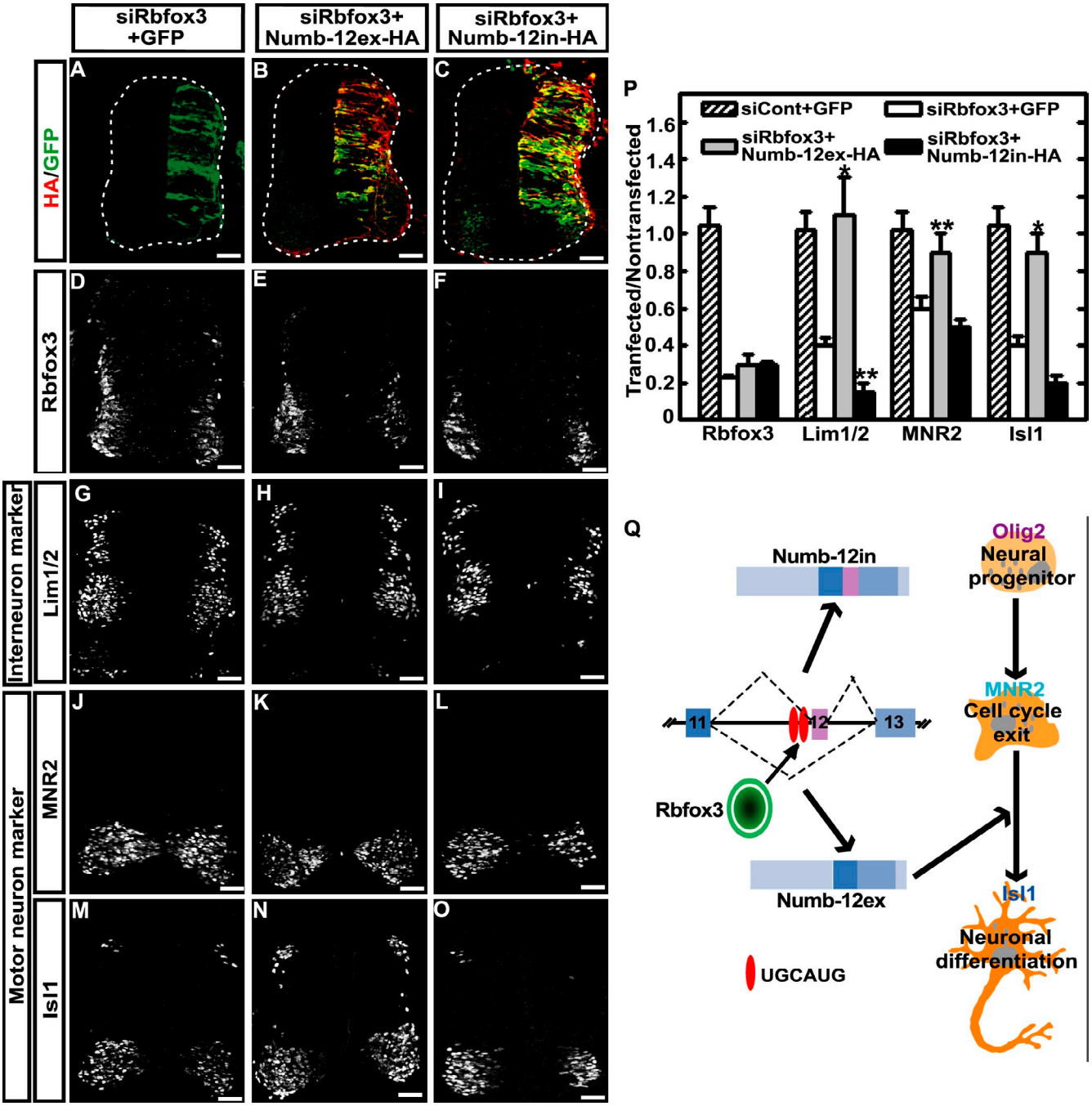

Figure 9. **Isoform-specific rescue of Rbfox3 knockdown–induced defects in neuronal differentiation by the Numb-12ex isoform.** (A–O) Immunostaining of the E4 neural tube for neuronal markers. The right side of the neural tube in each panel has been transfected with *siRbfox3* and the indicated expression construct, as demonstrated by GFP and HA-tagged Numb immunostaining in A–C. Both Numb-12ex-HA and Numb-12in-HA exclude exon 6. Bars, 50 µm. (P) Quantification of marker$^+$ cells. Quantification was performed by the same procedure as in Fig. 4 K (mean ± SD, 5 embryos, 3 sections/embryo). *, $P < 0.0001$; **, $P < 0.001$ compared with *siRbfox3+GFP*. (Q) A model for the Rbfox3-mediated regulation of neuronal development. Upon cell cycle exit, (MNR2 expressed) postmitotic neuronal cells express Rbfox3. Rbfox3 binds to the UGCAUG elements on the *Numb* premRNA and represses exon 12 usage. The resulting Numb-12ex isoform plays an isoform-specific role in promoting neuronal differentiation (Isl1 expression) of postmitotic neurons. Motor neuron markers are used as examples for states of differentiation.

with *Numb-12in* failed to rescue the defective neuronal differentiation in the Rbfox3-full knockdown embryos (Fig. 9, G vs. I, J vs. L, M vs. O; P). Rather, co-electroporation appeared to enhance the inhibition of differentiation marker expression, presumably reflecting multiple effects of Numb-12in on spinal neuronal development.

Collectively, we propose a model in which Rbfox3-full plays a critical role in the advancement of neuronal differentiation in postmitotic neurons by changing Numb isoforms from Numb-12in to Numb-12ex. Numb-12ex is specifically required for neuronal differentiation and Numb-12in cannot replace Numb-12ex function. Thus, the Numb isoform switch by

alternative premRNA splicing is directly regulated by Rbfox3 and is a key event in Rbfox3-mediated neuronal differentiation (Fig. 9 Q).

Discussion

Splice variants of Rbfox3

All three *Rbfox* genes have been shown to generate alternatively spliced variants of coding sequence in mammals (Nakahata and Kawamoto, 2005; Underwood et al., 2005; Kim et al., 2009). The cassette type alternative 93-nt RRM exon is highly conserved among paralogues. The RRM-defective isoforms of mouse Rbfox1 and Rbfox2 equivalent to chicken Rbfox3-d31 are expressed in a tissue- or cell type–dependent manner. These isoforms do not bind to the RNA element and are capable of acting as dominant-negative factors in some contexts (Nakahata and Kawamoto, 2005; Baraniak et al., 2006; Damianov and Black, 2010). Here we demonstrate that alternative splicing of the 93-nt RRM exon is regulated in a developmental stage–dependent manner. E2 chicken embryos, where only very limited numbers of postmitotic neurons are generated, already express *Rbfox3* mRNAs at a level similar to E4 embryos. This suggests that proliferating progenitor cells express *Rbfox3* mRNAs. However, essentially all *Rbfox3* mRNAs in E2 embryos exclude the 93-nt RRM exon and encode the d31 isoform. The Rbfox3-d31 protein is subject to rapid degradation. In contrast, *Rbfox3-full* mRNA encodes a stable protein and expression of this isoform increases from E3 onward and accumulates in postmitotic neurons. Therefore, alternative splicing of the 93-nt RRM exon is used as part of the mechanism for postmitotic neuron-restricted expression of Rbfox3 in chicken. Interestingly, the chicken intron downstream of the 93-nt RRM exon contains three copies of the UGCAUG element (Fig. S1 H). Based on the location of UGCAUG elements relative to the alternative exon, the 93-nt RRM exon of chicken *Rbfox3* would be activated by full-length Rbfox3, Rbfox1, or Rbfox2.

Neuronal differentiation defects due to Rbfox3 knockdown

Deficiency of Rbfox3-full in the developing spinal cord results in inhibition of late neuronal differentiation in postmitotic neurons without affecting neuronal fate and subtype specification of progenitor cells in the VZ and intermediate zone. The inhibition of induction of neuronal subtype-specific transcription factors (MNR2, Isl1, and Lim1/2) by Rbfox3 knockdown occurs in both motor neurons and interneurons in the entire MZ, and is associated with inhibition of expression of general neuronal proteins such as β-tubulin III. Therefore, Rbfox3 appears to participate in a general differentiation program in neurons. Supporting this notion, we found inhibition of neuronal differentiation of retinoic acid–treated P19 cells by Rbfox3 knockdown.

Despite a nearly 80% reduction in Rbfox3 expression in vivo, reductions in the expression of differentiated neuronal markers are rather mild (40–60%). This could be explained by a number of possibilities. First, other paralogues (Rbfox1 and Rbfox2) could compensate for the lack of Rbfox3. In the adult mouse CNS, Rbfox3-expressing neurons usually express Rbfox1 and 2 (Kim et al., 2011). Because the three paralogues share common structural and biochemical properties, they could share common targets of splicing regulation. Indeed, we observed a slight increase in *Rbfox1* mRNA expression in *siRbfox3*-transfected cells. Second, alternative splicing of premRNAs is regulated by multiple factors in a combinatorial manner. Deletion of one factor does not necessarily effect a complete change in splicing patterns. In many cases it changes only the frequency of a choice of splicing pattern and therefore the required splice isoform could be generated to a lower extent in the absence of Rbfox3. Heterologous ribonuclear proteins have been shown to co-regulate alternative splicing with Rbfox proteins in a number of cases (Li et al., 2007; Mauger et al., 2008). Recent bioinformatic studies predict a combinatorial regulation by Nova and Rbfox proteins for a set of alternative splicing events including mouse *Numb* exon 12 (Zhang et al., 2010). Third, the difference in biological activity between two splice isoforms could be quantitative rather than all-or-none or antagonistic to each other. In this case, a mis-expressed splice isoform in the Rbfox3 knockdown neural tube would have partial function.

Identification of *Numb* premRNA as a relevant target of Rbfox3 in the developing spinal cord

Our study established that *Numb* alternative splicing is a physiologically important target for Rbfox3 action during neuronal differentiation in the developing spinal cord in the period between E2 and E4. The findings that the isoform-specific knockdown of Numb-12ex leads to neuronal differentiation defects similar to those due to Rbfox3 knockdown and that the Numb-12ex isoform (but not Numb-12in) rescues the differentiation defects induced by Rbfox3 knockdown support our conclusion. However, our study does not exclude the possible existence of other Rbfox3 targets, especially during other developmental times, or in other neuronal subtypes, or during other neuronal activities. A recent study with Nova2 knockout mice reported that *Disabled1* is the only relevant splicing target of Nova2 for proper migration of neurons in the developing cortex during the period between E14.5 and E16.5 (Yano et al., 2010). In both cases, Rbfox3 in chick neural tube and Nova2 in developing mouse cortex, the cells are in the process of differentiation or migration before intensive synaptogenesis begins. In contrast, analyses of Nova2, Rbfox1, and Rbfox2 targets in adult brains have identified a number of sets of functionally related genes that mediate synaptic transmission and membrane excitation (Ule et al., 2005; Gehman et al., 2011, 2012). Although the functional importance of these splicing events has not been experimentally evaluated, coordinated regulation of a large number of targets presumably reflects a requirement for functionally diverse protein isoforms in the mature CNS. This is understandable because the CNS contains several hundred distinct types and subtypes of neurons. Moreover, coordinated intracellular activities of multiple proteins and coordinated intercellular activities of neurons are required for the operation of complicated neural circuits. One such example has been reported in *Nova*-null mice (Ruggiu et al., 2009).

Potential functions of Numb during spinal cord development

Numb contains a number of domains including a highly conserved phosphotyrosine-binding domain in the N terminus and DPF and NPF motifs for binding to endocytic proteins at the end of the C terminus. The C-terminal half of the vertebrate Numb molecule is the PRR containing a putative Src homology 3–binding site (Gulino et al., 2010). Alternative exon 12 encodes a part of the PRR. Our studies demonstrate that a switch in Numb isoforms from the exon 12–included to the exon 12–excluded isoform occurs during the transition from proliferating progenitor to differentiating neuron and the Numb-12ex isoform is required for progression of neuronal differentiation in postmitotic cells. These observations are consistent with a previous study showing distinctive functions of the two Numb isoforms in neuronal cultures; the Numb-12ex isoform promoted neuronal differentiation, whereas the Numb-12in isoform promoted cell proliferation (Verdi et al., 1999).

How does Numb-12ex regulate neuronal differentiation? Numb was first shown to regulate neuronal cell fate by inhibiting Notch signaling in *Drosophila* sensory organs (Guo et al., 1996). This finding has been extended to neurogenesis in the vertebrate CNS (Wakamatsu et al., 1999; Shen et al., 2002; Petersen et al., 2006). Therefore, we asked whether the Notch signaling pathway is mis-regulated in the Rbfox3 knockdown chick neural tube. In situ detection of *Notch1* mRNA as well as *Hes1* and *Hes5* mRNAs, the expression of which is known to be activated by Notch (Kaltezioti et al., 2010), showed that these mRNAs were confined to the VZ at E4 and that Rbfox3 knockdown has no effect (Fig. S2, Q–S). Therefore, Rbfox3-regulated neuronal differentiation appears to be independent of Notch signaling.

More recent studies on Numb have uncovered its participation in a wide range of membrane receptor signaling pathways including integrins, cadherins, and tyrosine kinase receptors (Rasin et al., 2007; Gulino et al., 2010; Pece et al., 2011; Zhou et al., 2011). Numb in turn plays a role in many biological processes including cell migration, adhesion, and endocytosis. Of interest, we observed that the density of postmitotic cells in the medial motor domain versus the lateral motor domain in the Rbfox3 knockdown side of the neural tube is higher compared with the control side. This suggests that the lateral migration of Rbfox3 knockdown cells is slowed down. The finding that the medially accumulated cells express the early motor neuron marker MNR2 but not the later marker Isl1 suggests that neural differentiation is associated with neural cell migration in the early developing spinal cord. It also raises a possibility that extrinsic factor(s) might be required for advancing neuronal differentiation. The two Numb isoforms may play different roles during cell migration and in receiving extracellular signals. Numb's primary function is in interacting with enzymes, receptors, phosphorylated proteins, and other yet unidentified proteins via a number of its domains and in linking different activities of its interacting proteins. Thus, it is tempting to speculate that the protein(s) relevant to neuronal differentiation are likely to have different affinities for Numb-12in and Numb-12ex. Future studies will endeavor to identify such proteins in order to understand the mechanism of Numb-12ex–mediated regulation of neuronal differentiation at the molecular level.

Materials and methods

Database deposition

The sequences reported in this study have been deposited in the GenBank database with accession numbers JN638312 (*Rbfox3-full*), JN638313 (*Rbfox3-d31*), JN638314 (*Numb-12in*), JN638315 (*Numb-12ex*), and JN638311 (partial genomic sequence of the chicken *Rbfox3* gene).

cDNA and genomic DNA cloning and construction of expression plasmids and minigenes

Rapid amplification of cDNA ends for chicken *Rbfox3* was performed using a GeneRacer kit (Invitrogen) and primers 5′-CCGGGCTGTGGCGTTGTTCACAATCTT-3′ and 5′-GCTTCTCTCGTGCCCGGTCGGCATCTG-3′ for the 5′ ends and 5′-CCGGGACCCCGACCTGCGGCAAATGTT-3′ and 5′-CGGGCAATTCGGGAAGATCCTGGATGT-3′ for the 3′ ends. The full-length coding regions of the chicken *Rbfox3* cDNAs (*Rbfox3-full* and *Rbfox3-d31*) were obtained by RT-PCR using total RNAs from E5 embryos and primers 5′-cccggggaattcGATGGCACAGCCCTACCCCCCGGCA-3′ and 5′-cccgggtctagaCAGAAGGAAAACGGCTGCGTGTTCA-3′. Lowercase letters represent adapter sequences including restriction enzyme sites (underlined). The EcoRI and XbaI fragments of the cDNAs were cloned into the plasmid pCS3+MT, which contains the cytomegalovirus (CMV) promoter and six copies of a myc epitope. The cDNA inserts cut out from the pCS3+MT construct by EcoRI and SnaBI were transferred into another expression plasmid pCIG4, which contains the chicken β-actin promoter with a CMV enhancer, a hemagglutinin epitope, and an internal ribosome entry site (ires) followed by the *EGFP* coding sequence, using EcoRI and SmaI sites. pCIG4 was a gift from T. Maynard (University of North Carolina, Chapel Hill, NC).

The full-length coding regions of the chicken *Numb* cDNAs (*Numb-12in* and *Numb-12ex*) were obtained by RT-PCR using total RNAs from E2 and E5 embryos and primers 5′-gggcccgaattcGAGAAATGAATAAATTACGGCAG-3′ and 5′-ggccggatcccgAAGTTCAATCTCAAATGTCTTCTGTAA-3′. The EcoRI and BamHI fragments of the cDNAs were cloned into the pCIG4 plasmid. The expression constructs encoding myc-smRbfox3-L and -S were previously described as myc-smFox-3-L and -S, respectively (Kim et al., 2011). Mouse *smRbfox3-L* and *-S* in the pCS3+MT plasmid contains the silent mutations at the region targeted by the *Rbfox3-T2* shRNA (OriGene, Kim et al., 2009); 5′-CGCACAGACTCATCCTGAGCAGCCAGGCA-3′ was changed to 5′-GGCTCAAACACACCCAGAACAACCTGGCA-3′.

Chicken genomic DNA including the 93-nt RRM exon of *Rbfox3* was amplified by PCR using primers 5′-CAATTCGGGAAGATCCTGGATGTGGAG-3′, 5′-CATTTTCAATGAGCGGGGCTCCAAG-3′, 5′-GGGTTTGCAGTCTTCTTGTTCGTCAT-3′, and 5′-CACCCGGGCTGTGGCGTTGTTCAC-3′, and cloned into the pCR2.1 vector using a TOPO cloning kit (Invitrogen).

Chicken genomic DNA including exons 11, 12, and 13 of the *Numb* gene was first obtained by PCR using primers 5′-ggatccgaattcTAACCGACTTGAAATTCGGAACACT-3′ and 5′-gcggccgcaagcttCGGCGGCTGCTGCCTGGGAAGCGGC-3′. The 2,820-bp EcoRI and HindIII fragment of this PCR product was cloned in the pET28 vector (EMD Millipore). The exon trap cloning plasmid pET01, which contains the Rous sarcoma virus long terminal repeat promoter and part of the rat *preproinsulin* gene with a polyadenylation signal, was used as a host vector for the minigene construction (Kawamoto, 1996). The 1,670-bp *Numb* genomic fragment including exon 11, intron 11, exon 12, and the flanking regions was cut out from the pET28 construct using BamHI and AflIII (blunt-ended) and inserted into the BamHI and NotI (blunt-ended) sites located in an intron between exons 2 and 3 of the *preproinsulin* gene. The TGCATG sequences at the 5′ and 3′ sides were changed to GTTACT and ACCTAC, respectively, by recombinant PCR.

siRNAs

The sense sequences of siRNAs are as follows: *siRbfox3*, 5′-CGAGAGAAGCUGAAUGGCAuu-3′ and 5′-GGGUUUGUAACUUUUGAAAuu-3′; *siN12in*, 5′-CAGCUAUGCCAGUUCGUGAuu-3′ and 5′-CUGUGUGCUUGCUGCUAAAuu-3′; *siN12ex*, 5′-CAAGGCACCGAAUGGAACAuu-3′ and 5′-CUUUCAAGGCACCGAAUGGuu-3′ (Thermo Fisher Scientific). *siCont* was obtained from Santa Cruz Biotechnology, Inc. (control siRNA-A sc-37007).

Chick in ovo electroporation, cell culture and transfection

In ovo electroporation was performed according to Rao et al. (2004). In brief, fertilized chicken eggs were incubated at 38°C until Hamburger Hamilton stage 11–13 (E2) before electroporation. Mixtures of DNA (each 100 ng/µl) and siRNA (each 100 ng/µl) were injected into the central canal of the neural tube and electroporation was performed with five pulses at 25 V, 50 ms each. After additional incubation at 38°C, embryos were fixed with 4% paraformaldehyde in phosphate-buffered saline for 1 h for immunostaining or overnight for in situ hybridization, and embedded in Optimal Cutting Temperature Compound (Sakura) in liquid nitrogen. In general, cryosections of the thoracic segment of the spinal cord were analyzed. Embryos for Figs. 3, 4, 7, 8, and 9 and Fig. 5, M–R were harvested at E4, and embryos for Fig. 5, A–L were harvested at E3.

Human SK-N-SH cells and mouse P19 cells were cultured and transfected with plasmids and siRNAs as described previously (Kim et al., 2009). *ShRbfox3-T2* and *shRbfox3-T3* are the same as shRNA *T-2* and *T-3*, respectively, in the previous publication. Neural differentiation of P19 cells was induced by retinoic acid as described previously (Kim et al., 2009). In brief, cells were cultured in a bacterial-grade Petri dish in a medium containing 5×10^{-7} M all-trans retinoic acid for 4 d. The cell aggregates were resuspended by mild pipetting and trypsin/EDTA treatment. The resuspended cells were then transferred to a poly-D-lysine–coated tissue culture dish and cultured for an additional 4 d. For rescue experiments shown in Fig. 1 N, the *Rbfox3* expression plasmids were transfected into clonal shRNA expressing cells by electroporation (Amaxa Nucleofector) after the 4-d retinoic acid treatment and before replating cells on a poly-D-lysine–coated dish.

Preparation of extracts and immunoblot analysis

Embryo and cell extracts were prepared using a radioimmunoprecipitation assay buffer (Sigma-Aldrich) supplemented with a protease inhibitor cocktail (P8340; Sigma-Aldrich). Gel electrophoresis and immunoblotting were performed as described previously (Kim et al., 2009). Antibodies used were mouse anti-phosphorylated neurofilaments (1:1,000, SMI-310R; Covance), mouse anti-Tuj1 (1:1,000, MMS-435P; Covance), goat anti-Numb (1:1,000, ab4147; Abcam), mouse anti-GAPDH (1:5,000, H86504M; Biodesign), mouse anti-myc (1:5,000, 46–0603; Invitrogen), and rabbit anti-Rbfox2 sera raised against GST-fused mouse Rbfox2 aa1-112 (1:5,000; Kim et al., 2011). Rabbit anti-Rbfox3 sera against mouse Rbfox3 aa 1–97 (1:3,000; Kim et al., 2009) and mouse anti-Rbfox3 (1:500, anti-NeuN, MAB377; EMD Millipore) were used for Fig. 1 M and Fig. 2 C, respectively.

FACS analysis

Chick trunks were dissected and passed through a cell strainer (pore size, 40 µm) to prepare a single cell suspension. The cells were washed in phosphate-buffered saline containing bovine serum albumin, an RNase inhibitor (Roche), and a protease inhibitor cocktail (Sigma-Aldrich). The cells were analyzed and sorted by GFP signal using a MoFlo cell sorter (Cytomation, Inc.). Pooled GFP^+ cells were used for RNA extraction.

RNA preparation and RT-PCR

Total RNA was isolated from chicken embryos and cultured cells using an RNeasy Mini kit (QIAGEN). The PCR primers used were 5′-CATTTTCAATGAGCGGGGGCTCCAA-3′ (P1) and 5′-CATGACCCTCTACACACCAGCACA-3′ (P2) for the *Rbfox3* 93-nt RRM exon region, 5′-CCTCATCAGTGGCAGACTGATGAAGAAGG-3′ (P3) and 5′-CTGACACCCACAGGACCGCTTTAACCGCC-3′ (P4) for the *Numb* exon 6 region, 5′-TCCCAGAGGTGGAAGGGGAAGTGGACAGC-3′ (P5) and 5′-CCTCTGAGGGAGTACGTCTGTGATTTCC-3′ (P6) for the *Numb* exon 12 region, 5′-CAAATCACAGCCAAAACGGCTTCACGTC-3′ and 5′-CTGCACCAACTGGATTTAATTTCCAG-3′ for *Rbfox1*, 5′-CCACTCCAAAACGACTTCATGTGTCTAAC-3′ and 5′-CGTACACCGCTCCAACCACAGGACTCAAC-3′ for *Rbfox2*, and 5′-CTGGCACCTAGCACAATGAA-3′ and 5′-CTGCTTGCTGATCCACATCT-3′ for *β-actin*. The primers to detect the *Numb* minigene mRNAs were 5′-GTGGATTCTTCTACACACCCAT-3′ (P11) and 5′-CCTCCACCCAGCTCCAGTTGT-3′ (P12). The primers to detect the *NMHCII-B* minigene mRNAs were described previously (Nakahata and Kawamoto, 2005).

RNA–protein complex immunoprecipitation

RNA–protein complexes were immunoprecipitated using a Magna RIP kit (EMD Millipore) according to the manufacturer's instructions. The RNAs recovered from the complexes were subjected to RT-PCR using primers 5′-CCTTCCCTAATCCCAGATTTATGAGAC-3′ (P9) and 5′-CTACAATGGAGCAGACAACATGGATGG-3′ (P10) for the *Numb* intronic region. The PCR program using P9 and P10 consists of 38 cycles of 94°C for 30 s, 58°C for 30 s, 72°C for 50 s. As a nonspecific control, *Numb* mRNAs were amplified using P5 and P6 in a PCR program consisting of 33 cycles of 94°C for 30 s, 52°C for 30 s, 72°C for 50 s.

RNA–protein UV cross-linking

Template DNAs for in vitro RNA transcription were prepared by PCR using the wild-type and mutant UISs in the minigenes as templates with primers 5′-TAATACGACTCACTATAGGGATTTGGCTAATTTACGCAAAC-3′ and 5′-CTAAAATGGGAGCAGACAACATCAGT-3′. The upstream primer included the T7 promoter sequence (underlined) at the 5′ end. The 146-nt RNAs were transcribed by T7 RNA polymerase in the presence of α-[^{32}P]UTP using a MAXIscript kit (Ambion). Quality and quantity of RNA probes were verified by gel electrophoresis using a Urea/10% polyacrylamide gel. Myc-Rbfox3 protein was synthesized in vitro from the pCS3+MT construct using the TNT Coupled Reticulocyte Lysate System (Promega). Binding reactions were performed in a 25-µl mixture that contains 10 mM Hepes, pH 7.9, 2 mM $MgCl_2$, 1 mM ATP, 20 mM creatine phosphate, 50 ng yeast tRNA, 2 mM DTT, 2% polyethylene glycol (mol wt 3,550), 4 µl of the reticulocyte lysate reaction mixture, and 10^6 cpm RNA probe for 20 min at 30°C. Reaction mixtures were irradiated with UV light (Stratalinker; Agilent Technologies) for 20 min on ice, digested with 2 µl RNase-A/T1 (Ambion) and immunoprecipitated with 2 µg of anti-myc. Samples were subject to SDS-PAGE and the radiolabeled RNAs bound to myc-Rbfox3 were visualized by autoradiography.

In situ hybridization and image acquisition

Total *Numb* and *Numb-12ex*-specific mRNAs were detected using biotinylated oligonucleotide probes (Bioneer Inc.) 5′ biotin-TTCGCAAGGACAGCTGGCGCTTAAAAGGAGACATCTTTTGACTAAGGGCAGGGAAGCCCC-3′ (P7) and 5′ biotin-TGCCGGGGGTGCTGCTGTTCCATTCGGTGCCTTGAAAGGCAGGAGACTGTGGGGCGACCA-3′ (P8), respectively. Hybridization and detection were performed using an IsHyb In Situ Hybridization kit (Biochain Institute, Inc.) and a DNADetector System (KPL, Inc.) according to the manufacturers' protocols.

The chicken *NeuroD4* and *Neurogenin2* cDNAs including the full-length coding sequences were obtained by RT-PCR using primers 5′-CCTCGTTACAGAGCTGAGAGATGAC-3′ and 5′-CCCGCTTCGCTACTCGTTGAAGATG-3′ (*NeuroD4*), and 5′-CGCAGGATGCCGGTGAAGGCGGAGAG-3′ and 5′-CTCGTAAATCACGGAGACAGCTGCG-3′ (*Neurogenin2*). The cDNAs were cloned in the pCRII-TOPO vector (Invitrogen) and were used as templates to prepare antisense RNA probes. Other constructs to prepare probes for chicken *NeuroD* and *Neurogenin2* were kindly provided by S.-K. Lee (Oregon Health and Science University, Portland, OR). The constructs used to prepare probes for *Notch1*, *Hes1*, and *Hes5* were kindly provided by P.K. Politis (Biomedical Research Foundation of the Academy of Athens, Athens, Greece). Antisense probes were synthesized using a DIG RNA labeling kit (Roche) and hybridized probes were detected using a BCIP/NBT Alkaline Phosphatase Substrate kit (Vector Laboratories).

The specimens were examined at RT using a light microscope (model BX40; Olympus) with a 10×/0.4 NA objective lens (Olympus) connected to a SPOT FLEX camera (Diagnostic Instruments, Inc.). Images were processed with Photoshop Elements 8.0 (Adobe).

Immunofluorescence microscopy and quantification

Freshly prepared cryosections were stained with the following primary antibodies: mouse anti-Rbfox3 (1:500, anti-NeuN, MAB377; EMD Millipore), rabbit anti-Olig2 (1:500, AB9610; EMD Millipore), mouse anti-p27kip1 (1:1,000, 610241; BD), mouse anti-phosphorylated neurofilaments (1:1,000, SMI-310R; Covance), rabbit anti-phosphohistone3 (1:100, 9701; Cell Signaling Technology), and rabbit anti-HA (1:1,000, SC-805; Santa Cruz Biotechnology, Inc.). Mouse anti-MNR2 (81.5C10), anti-Isl1 (40.3A4), anti-Lim1/2 (4F2), anti-Pax6 (PAX6), anti-Nkx6.1 (F55A10), and anti-Nkx2.2 (74.5A5) were obtained from Developmental Studies Hybridoma Bank (University of Iowa, Iowa City, IA) and used at a dilution of 1:20. Rabbit anti-Rbfox3 sera against mouse Rbfox3 aa 1–97 (1:2,000; Kim et al., 2009) was used for Fig. 1, D–L. Alexa Fluor 488– and 594–conjugated goat antibodies against mouse IgG and rabbit IgG (1:500; Molecular Probes) were used as secondary antibodies. Nuclear DNA was stained with DAPI (Sigma-Aldrich). TUNEL assay was performed using an In Situ Cell Death Detection kit (Roche). Specimens were mounted in ProLong Gold Antifade reagent (Invitrogen). Images were acquired at RT using a confocal laser-scanning microscope (LSM510 Meta; Carl Zeiss) with a Plan Neofluar 20×/0.5 NA air objective lens (Carl Zeiss). The acquisition software used was LSM510.

Cell (nuclear) numbers of transcription factor or DAPI-positive cells, regardless of staining intensities, were manually counted by enlarging images. The expression levels of Rbfox3 and β-tubulin III were quantified by fluorescence intensities using ImageJ software version 1.37 (National Institutes of Health, Bethesda, MD).

The border between TM and TL shown Fig. 4 L was defined as the mid-line of the width of the motor domain.

Online supplemental material

Fig. S1 shows comparison of chicken and mouse Rbfox3 sequences and properties of chicken Rbfox3 isoforms. Fig. S2 shows effects of Rbfox3-full knockdown in progenitor generation, proneural gene expression, and Notch signaling in the chick neural tube. Fig. S3 shows effects of forced expression of Rbfox3-full on progenitors in the VZ. Fig. S4 shows the conserved TGCATG element in the upstream intron of exon 12 in vertebrate *Numb* genes and effects of chicken and mouse Rbfox3 isoforms on exon 12 splicing of the *Numb* minigene. Fig. S5 shows effects of forced expression of Numb isoforms on neuronal differentiation in the chick neural tube. Online supplemental material is available at http://www.jcb.org/cgi/content/full/jcb.201206146/DC1.

We are grateful to R.S. Adelstein for continued encouragement, helpful advice, and comments on the manuscript. Thanks to C.A. Combs and D. Malide for invaluable help in confocal microscopy; L. Samsel and J.P. McCoy for FACS assistance; K. Gill for laboratory management and technical support; and Y. Carter and L. Oundo for administrative assistance. Thanks also to A.M. Michelson and J.M. James for helpful discussion; the members of Laboratory of Molecular Cardiology and Laboratory of Stem Cell and Neuro-Vascular Biology for technical help and thoughtful discussion; and M.A. Conti for critical reading of the manuscript.

This work was supported by the Division of Intramural Research, National Heart, Lung, and Blood Institute, NIH.

Submitted: 29 June 2012
Accepted: 23 January 2013

References

Auweter, S.D., R. Fasan, L. Reymond, J.G. Underwood, D.L. Black, S. Pitsch, and F.H. Allain. 2006. Molecular basis of RNA recognition by the human alternative splicing factor Fox-1. *EMBO J.* 25:163–173. http://dx.doi.org/10.1038/sj.emboj.7600918

Baraniak, A.P., J.R. Chen, and M.A. Garcia-Blanco. 2006. Fox-2 mediates epithelial cell-specific fibroblast growth factor receptor 2 exon choice. *Mol. Cell. Biol.* 26:1209–1222. http://dx.doi.org/10.1128/MCB.26.4.1209-1222.2006

Briscoe, J., and B.G. Novitch. 2008. Regulatory pathways linking progenitor patterning, cell fates and neurogenesis in the ventral neural tube. *Philos. Trans. R. Soc. Lond. B Biol. Sci.* 363:57–70. http://dx.doi.org/10.1098/rstb.2006.2012

Damianov, A., and D.L. Black. 2010. Autoregulation of Fox protein expression to produce dominant negative splicing factors. *RNA*. 16:405–416. http://dx.doi.org/10.1261/rna.1838210

Dredge, B.K., and K.B. Jensen. 2011. NeuN/Rbfox3 nuclear and cytoplasmic isoforms differentially regulate alternative splicing and nonsense-mediated decay of Rbfox2. *PLoS ONE*. 6:e21585. http://dx.doi.org/10.1371/journal.pone.0021585

Fagnani, M., Y. Barash, J.Y. Ip, C. Misquitta, Q. Pan, A.L. Saltzman, O. Shai, L. Lee, A. Rozenhek, N. Mohammad, et al. 2007. Functional coordination of alternative splicing in the mammalian central nervous system. *Genome Biol.* 8:R108. http://dx.doi.org/10.1186/gb-2007-8-6-r108

Gehman, L.T., P. Stoilov, J. Maguire, A. Damianov, C.H. Lin, L. Shiue, M. Ares Jr., I. Mody, and D.L. Black. 2011. The splicing regulator Rbfox1 (A2BP1) controls neuronal excitation in the mammalian brain. *Nat. Genet.* 43:706–711. http://dx.doi.org/10.1038/ng.841

Gehman, L.T., P. Meera, P. Stoilov, L. Shiue, J.E. O'Brien, M.H. Meisler, M. Ares Jr., T.S. Otis, and D.L. Black. 2012. The splicing regulator Rbfox2 is required for both cerebellar development and mature motor function. *Genes Dev.* 26:445–460. http://dx.doi.org/10.1101/gad.182477.111

Gulino, A., L. Di Marcotullio, and I. Screpanti. 2010. The multiple functions of Numb. *Exp. Cell Res.* 316:900–906. http://dx.doi.org/10.1016/j.yexcr.2009.11.017

Guo, M., L.Y. Jan, and Y.N. Jan. 1996. Control of daughter cell fates during asymmetric division: interaction of Numb and Notch. *Neuron*. 17:27–41. http://dx.doi.org/10.1016/S0896-6273(00)80278-0

Jessell, T.M. 2000. Neuronal specification in the spinal cord: inductive signals and transcriptional codes. *Nat. Rev. Genet.* 1:20–29. http://dx.doi.org/10.1038/35049541

Jin, Y., H. Suzuki, S. Maegawa, H. Endo, S. Sugano, K. Hashimoto, K. Yasuda, and K. Inoue. 2003. A vertebrate RNA-binding protein Fox-1 regulates tissue-specific splicing via the pentanucleotide GCAUG. *EMBO J.* 22:905–912. http://dx.doi.org/10.1093/emboj/cdg089

Kaltezioti, V., G. Kouroupi, M. Oikonomaki, E. Mantouvalou, A. Stergiopoulos, A. Charonis, H. Rohrer, R. Matsas, and P.K. Politis. 2010. Prox1 regulates the notch1-mediated inhibition of neurogenesis. *PLoS Biol.* 8:e1000565. http://dx.doi.org/10.1371/journal.pbio.1000565

Kawamoto, S. 1996. Neuron-specific alternative splicing of nonmuscle myosin II heavy chain-B pre-mRNA requires a cis-acting intron sequence. *J. Biol. Chem.* 271:17613–17616.

Kim, K.K., R.S. Adelstein, and S. Kawamoto. 2009. Identification of neuronal nuclei (NeuN) as Fox-3, a new member of the Fox-1 gene family of splicing factors. *J. Biol. Chem.* 284:31052–31061. http://dx.doi.org/10.1074/jbc.M109.052969

Kim, K.K., Y.C. Kim, R.S. Adelstein, and S. Kawamoto. 2011. Fox-3 and PSF interact to activate neural cell-specific alternative splicing. *Nucleic Acids Res.* 39:3064–3078. http://dx.doi.org/10.1093/nar/gkq1221

Kuroyanagi, H., G. Ohno, S. Mitani, and M. Hagiwara. 2007. The Fox-1 family and SUP-12 coordinately regulate tissue-specific alternative splicing in vivo. *Mol. Cell. Biol.* 27:8612–8621. http://dx.doi.org/10.1128/MCB.01508-07

Lee, S.K., and S.L. Pfaff. 2003. Synchronization of neurogenesis and motor neuron specification by direct coupling of bHLH and homeodomain transcription factors. *Neuron*. 38:731–745. http://dx.doi.org/10.1016/S0896-6273(03)00296-4

Li, Q., J.A. Lee, and D.L. Black. 2007. Neuronal regulation of alternative pre-mRNA splicing. *Nat. Rev. Neurosci.* 8:819–831. http://dx.doi.org/10.1038/nrn2237

Maris, C., C. Dominguez, and F.H. Allain. 2005. The RNA recognition motif, a plastic RNA-binding platform to regulate post-transcriptional gene expression. *FEBS J.* 272:2118–2131. http://dx.doi.org/10.1111/j.1742-4658.2005.04653.x

Mauger, D.M., C. Lin, and M.A. Garcia-Blanco. 2008. hnRNP H and hnRNP F complex with Fox2 to silence fibroblast growth factor receptor 2 exon IIIc. *Mol. Cell. Biol.* 28:5403–5419. http://dx.doi.org/10.1128/MCB.00739-08

McKee, A.E., E. Minet, C. Stern, S. Riahi, C.D. Stiles, and P.A. Silver. 2005. A genome-wide in situ hybridization map of RNA-binding proteins reveals anatomically restricted expression in the developing mouse brain. *BMC Dev. Biol.* 5:14. http://dx.doi.org/10.1186/1471-213X-5-14

Mullen, R.J., C.R. Buck, and A.M. Smith. 1992. NeuN, a neuronal specific nuclear protein in vertebrates. *Development*. 116:201–211.

Nakahata, S., and S. Kawamoto. 2005. Tissue-dependent isoforms of mammalian Fox-1 homologs are associated with tissue-specific splicing activities. *Nucleic Acids Res.* 33:2078–2089. http://dx.doi.org/10.1093/nar/gki338

Pece, S., S. Confalonieri, P. R Romano, and P.P. Di Fiore. 2011. NUMB-ing down cancer by more than just a NOTCH. *Biochim. Biophys. Acta*. 1815:26–43.

Petersen, P.H., H. Tang, K. Zou, and W. Zhong. 2006. The enigma of the numb-Notch relationship during mammalian embryogenesis. *Dev. Neurosci.* 28:156–168. http://dx.doi.org/10.1159/000090761

Ponthier, J.L., C. Schluepen, W. Chen, R.A. Lersch, S.L. Gee, V.C. Hou, A.J. Lo, S.A. Short, J.A. Chasis, J.C. Winkelmann, and J.G. Conboy. 2006. Fox-2 splicing factor binds to a conserved intron motif to promote inclusion of protein 4.1R alternative exon 16. *J. Biol. Chem.* 281:12468–12474. http://dx.doi.org/10.1074/jbc.M511556200

Rao, M., J.H. Baraban, F. Rajaii, and S. Sockanathan. 2004. In vivo comparative study of RNAi methodologies by in ovo electroporation in the chick embryo. *Dev. Dyn.* 231:592–600. http://dx.doi.org/10.1002/dvdy.20161

Rasin, M.R., V.R. Gazula, J.J. Breunig, K.Y. Kwan, M.B. Johnson, S. Liu-Chen, H.S. Li, L.Y. Jan, Y.N. Jan, P. Rakic, and N. Sestan. 2007. Numb and Numbl are required for maintenance of cadherin-based adhesion and polarity of neural progenitors. *Nat. Neurosci.* 10:819–827. http://dx.doi.org/10.1038/nn1924

Ruggiu, M., R. Herbst, N. Kim, M. Jevsek, J.J. Fak, M.A. Mann, G. Fischbach, S.J. Burden, and R.B. Darnell. 2009. Rescuing Z+ agrin splicing in Nova null mice restores synapse formation and unmasks a physiologic defect in motor neuron firing. *Proc. Natl. Acad. Sci. USA*. 106:3513–3518. http://dx.doi.org/10.1073/pnas.0813112106

Shen, Q., W. Zhong, Y.N. Jan, and S. Temple. 2002. Asymmetric Numb distribution is critical for asymmetric cell division of mouse cerebral cortical stem cells and neuroblasts. *Development*. 129:4843–4853.

Tanabe, Y., C. William, and T.M. Jessell. 1998. Specification of motor neuron identity by the MNR2 homeodomain protein. *Cell*. 95:67–80. http://dx.doi.org/10.1016/S0092-8674(00)81783-3

Ule, J., A. Ule, J. Spencer, A. Williams, J.S. Hu, M. Cline, H. Wang, T. Clark, C. Fraser, M. Ruggiu, et al. 2005. Nova regulates brain-specific splicing to shape the synapse. *Nat. Genet.* 37:844–852. http://dx.doi.org/10.1038/ng1610

Underwood, J.G., P.L. Boutz, J.D. Dougherty, P. Stoilov, and D.L. Black. 2005. Homologues of the *Caenorhabditis elegans* Fox-1 protein are neuronal splicing regulators in mammals. *Mol. Cell. Biol.* 25:10005–10016. http://dx.doi.org/10.1128/MCB.25.22.10005-10016.2005

Verdi, J.M., A. Bashirullah, D.E. Goldhawk, C.J. Kubu, M. Jamali, S.O. Meakin, and H.D. Lipshitz. 1999. Distinct human NUMB isoforms regulate differentiation vs. proliferation in the neuronal lineage. *Proc. Natl. Acad. Sci. USA*. 96:10472–10476. http://dx.doi.org/10.1073/pnas.96.18.10472

Wakamatsu, Y., T.M. Maynard, S.U. Jones, and J.A. Weston. 1999. NUMB localizes in the basal cortex of mitotic avian neuroepithelial cells and modulates neuronal differentiation by binding to NOTCH-1. *Neuron*. 23:71–81. http://dx.doi.org/10.1016/S0896-6273(00)80754-0

Yano, M., Y. Hayakawa-Yano, A. Mele, and R.B. Darnell. 2010. Nova2 regulates neuronal migration through an RNA switch in disabled-1 signaling. *Neuron*. 66:848–858. http://dx.doi.org/10.1016/j.neuron.2010.05.007

Yeo, G.W., N.G. Coufal, T.Y. Liang, G.E. Peng, X.D. Fu, and F.H. Gage. 2009. An RNA code for the FOX2 splicing regulator revealed by mapping RNA-protein interactions in stem cells. *Nat. Struct. Mol. Biol.* 16:130–137. http://dx.doi.org/10.1038/nsmb.1545

Zhang, C., Z. Zhang, J. Castle, S. Sun, J. Johnson, A.R. Krainer, and M.Q. Zhang. 2008. Defining the regulatory network of the tissue-specific splicing factors Fox-1 and Fox-2. *Genes Dev.* 22:2550–2563. http://dx.doi.org/10.1101/gad.1703108

Zhang, C., M.A. Frias, A. Mele, M. Ruggiu, T. Eom, C.B. Marney, H. Wang, D.D. Licatalosi, J.J. Fak, and R.B. Darnell. 2010. Integrative modeling defines the Nova splicing-regulatory network and its combinatorial controls. *Science*. 329:439–443. http://dx.doi.org/10.1126/science.1191150

Zhou, P., J. Alfaro, E.H. Chang, X. Zhao, M. Porcionatto, and R.A. Segal. 2011. Numb links extracellular cues to intracellular polarity machinery to promote chemotaxis. *Dev. Cell*. 20:610–622. http://dx.doi.org/10.1016/j.devcel.2011.04.006